

## สำนักงานกองทุนสนับสนุนการวิจัย THE THAILAND RESEARCH FUND

รายงานวิจัยฉบับสมบูรณ์

โครงการ 'Phase Behaviour of polyolefin Blends under Melt Flow'

โดย ดร. ริชาร์ด เว็นเนเบิลส์ และคณะ

31 กรกฏาคม 2546



# THE THAILAND RESEARCH FUND

รายงานวิจัยฉบับสมบูรณ์

โครงการ ' Phase Behaviour of polyolefin Blends under Melt Flow '

โดย ดร. ริชาร์ด เว็นเนเบิลส์ และคณะ

31 กรกฎาคม 2546

# รายงานวิจัยฉบับสมบูรณ์

โครงการ ' Phase Behaviour of polyolefin Blends under Melt Flow '

ดร. ริชาร์ด เว็นเนเบิลส์

ภาควิชาเคมี คณะวิทยาศาสตร์ มหาวิทยาลัยมหิดล

สนับสนุนโดยสำนักงานกองทุนสนับสนุนการวิจัย

(ความเห็นในรายงานนี้เป็นของผู้วิจัย สกว.ไม่จำเป็นต้องเห็นด้วยเสมอไป)

## กิตติกรรมประกาศ

ุ กณะผู้วิจัยขอขอบคุณสำนักงานกองทุนสนับสนุนการวิจัยที่ให้การทุนสนับสนุนงานวิจัยนี้

#### บทคัดย่อ

ระหัสโครงการ: BRG43-8-0012

ชื่อโครงการ: Phase Behaviour of polyolefin Blends under Melt Flow

นักวิจัย: ดร. ริชาร์ด เว็นเนเบิลส์

ภาควิชาเคมี คณะวิทยาศาสตร์ มหาวิทยาลัยมหิดล

frrav@mahidol.ac.th

ระยะเวลาโครงการ: สิงหาคม 2543 - กรกฎาคม 2546

### วัตถุประสงค์

- ศึกษาสัณฐานวัฏภาคในสถานะของแข็ง ที่เกิดจาก liquid-liquid phase separation ของพอลิเมอร์ผสม ระหว่างพอลิเอทิลีนชนิดสายโซ่ตรงกับ เอทิลีน-เอลฟา-โอลีฟิน โคพอลิเมอร์ ในการผสมขณะเกิดการใหล ที่ใช้ในการขึ้นรูป และเปรียบเทียบกับตัวอย่างที่ได้จากการเตรียมในสภาวะที่ไม่มีการไหล
- ศึกษาถึงรายละเอียด ความสัมพันธ์ระหว่างสภาวะที่เกิดการผสมกับสัณฐานวัฏภาคที่ได้ ศึกษาสมบัติ ทางฟิสิกส์ และวัดค่าที่เกี่ยวกับสมบัติทางฟิสิกส์
- การวิเคราะห์ ความสัมพันธ์ระหว่างโครงสร้างสัณฐานกับสมบัติเชิงกล ของพอลิเมอร์ผสมที่ไม่เข้ากัน จากสัณฐานวัฏภาคที่เกิดจาก liquid-liquid phase separation และการศึกษาสมบัติเชิงกลด้าน การแตกหัก (fracture mechanics)
- สุดท้ายจะเป็นการสร้างความสัมพันธ์ระหว่าง processing-morphology-property ของระบบนี้ เพื่อนำไป สู่การเตรียมคอมพาวด์ที่ดีที่สุด และอาจมีสัณฐานแบบใหม่ซึ่งนำไปสู่สมบัติเชิงกลที่ดีขึ้น

#### การทดลอง

เพื่อจะศึกษาผลของ thermomechanical history ต่อสัณฐานที่เกิดขึ้น เตรียมพอลิโอลิฟินผสมโดยการ เตรียมเป็นสารละลายผสม แล้วทำให้พอลิโอลิฟินผสมตกตะกอน ศึกษาการให้แรงเฉือนต่อตัวอย่างที่ได้ ที่ อุณหภูมิต่างๆ แล้วติดตามการเปลี่ยนแปลงของสัณฐานที่เกิดขึ้นหลังจากการให้ความร้อนในขณะหลอม เหลวแล้วทำให้เย็นตัวอย่างรวดเร็ว โดยการใช้ microscopy ศึกษาในลักษณะเป็นแผ่นบางๆที่ตัดจาก ตัวอย่าง หรือ จากผิวของตัวอย่างที่ผ่านการตัดให้เรียบ

#### ผลจากการทดลอง

การให้ความร้อนและงานกลในขั้นตอนการผสมและขึ้นรูปพอลิโอลิฟินผสม มีผลอย่างมากต่อ สัณฐานวัฏภาคที่เกิดขึ้นและสมบัติเชิงฟิสิกส์ของวัสดุ ผลของอุณหภูมิและแรงเฉือนจะแตกต่างกันในพอลิ-เมอร์ผสมแต่ละระบบ โดยจะขึ้นกับการเข้ากันได้ของพอลิเมอร์ที่เป็นส่วนผสม

ในระบบที่ผสมเข้ากันได้บางส่วน เช่น พอลิเมอร์ผสมระหว่าง พอลิเอทิลีน และ พอลิ(เอทิลีน-โค-1-ออกทีน) พบว่า การไหลขณะหลอมเหลวเป็นผลทำให้เกิดสัณฐานแบบ fine length-scale ซึ่งประกอบ ด้วย ลาเมลล่าของพอลิเอทีลีนแทรกอยู่ในส่วนที่เป็นพอลิ(เอทิลีน-โค-1-ออกทีน) ซึ่งเป็นสัณฐานที่เกิด จาก liquid-liquid และ liquid-solid phase separation พร้อมกัน โดยเกิดขึ้นในขณะที่ ของผสมหยุดใหลแล้วทำให้เย็น

จากการศึกษาในระบบที่ผสมเข้ากันได้บางส่วนพบว่า แรงเฉือนมีผลต่อ the superposition of time and temperature upon the coarsening process ที่พบได้จากตัวอย่างที่เดรียมโดยไม่มีแรงเฉือน พบว่าการให้แรงเฉือนขนาด 1 ต่อวินาที ต่อพอลิเมอร์ผสมที่มี 2 วัฎภาค มีผลต่อการเร่งอัตราการโตของ domain morphology เมื่อเปรียบเทียบกับ ตัวอย่างที่ไม่มีแรงเฉือนและ ที่ได้รับแรงเฉือนที่ 50 ต่อวินาที ในทุกกรณีพบว่าการให้ตัวอย่างอยู่ภายใต้อุณหภูมิสูงจะมีผลต่อการลดลงของอัตราการโต ช่วงการ annealing ในขั้นถัดไป นอกจากนั้นผลของอุณหภูมิสูงจะเพิ่มขึ้นเมื่อตัวอย่างได้รับแรงเฉือนที่ รุนแรงภายในขั้นดอน injection moulding แม้ว่าตัวอย่างอยู่ภายใต้อุณหภูมิสูงแค่เวลาช่วงสั้น แต่ก็จะ มีผลอย่างมากต่อสัณฐานที่จะเกิดขึ้นในการเตรียมตัวอย่างในขั้นถัดไป ผลที่เกิดขึ้นนี้ไม่ได้มาจากการ เปลี่ยนความหนึดของตัวอย่างที่หลอมเหลว ที่เป็นหลักฐานมาจากการไม่ซ้อนทับกันของข้อมูลที่ได้จาก การพิจารณาตาม the superposition of time and temperature สัณฐานที่ซับซ้อนเกิดขึ้นตอน หล่อตัวอย่างมาจากผลของการเข้ากันได้บางส่วนในขณะที่สารหลอมเหลว และ การแยกวัฏภาคที่เกิดขึ้น ขณะตัวอย่างเย็นลงและการเกิดผลึกขึ้น สัณฐานที่ได้มีผลต่อความเหนียวของวัสดุเมื่อรับแรงกระแทกที่ สัณฐานในตัวอย่างที่หยาบขึ้นที่มีผลมาจากการมีปริมาณของยางสูงขึ้น อณหภมิต่ำ ประกอบในพอลิเมอร์ผสมเข้ากันได้น้อยลงจะมีผลอย่างมากต่อการทนแรงกระแทกที่อุณหภูมิต่ำ

ระบบที่มีใอโชแทกติกพอลิโปรพิลีนกับ ไอโชแทกติกพอลิ(โปรพิลีน-โค-เอทิลีน) ซึ่งมีการผสม เข้ากันได้น้อยกว่าระบบที่มีพอลิเอทิลีน จะมีสมบัติการทนแรงกระแทกขึ้นกับ injection moulding condition อย่างวิกฤต โดยที่ความเหนียวจะลดลงเมือขนาดของยางใหญ่ขึ้นในการหล่อที่อุณหภูมิสูงขึ้น สำหรับตัวอย่างระบบพอลิเอทิลีนซึ่งมีการเข้ากันได้ดีในขณะที่สารหลอมเหลว การหล่อที่อุณหภูมิสูงต่าง กัน จะมีผลเพียงเล็กน้อยต่อความเหนียว

การที่มีโคพอลิเมอร์ที่มีสายโช่ผสมอยู่กับพอลิเอทิลีน จะมีผลทำให้การแตกหักของพอลิเอทิลีน แตกต่างกันโดยจะขึ้นกับทิศทางที่ทำการทดสอบตัวอย่าง พบว่าการเรียงตัวอย่างเป็นระเบียบของ พอลิเอทิลีนจะเป็นตัวกำหนดขบวนการแตกหักของตัวอย่างในทิศ TD ดังนั้นการที่มีพอล์ใเอทิลีน-โค-1-ออกทีน) รวมอยู่จึง มีผลเพียงเล็กน้อย ส่วนในทิศ MD โคพอลิเมอร์ที่มีสายโช่จะเพิ่ม non-essential work of fracture แต่จะ มีผลเล็กน้อยต่อ essential work of fracture

## สรุป

จากงานวิจัยนี้พบว่า processing history มีผลอย่างมากต่อสัณฐานที่ได้ของพอลิโอลิฟินผสม แรงเฉือนและอุณหภูมิมีผลอย่างวิกฤตต่อสัณฐานที่เกิดขึ้นจากขบวนการผสมหรือขึ้นรูปในขั้นต่อไป ใน บางกรณีมีผลทำให้ความเหนียวที่วัดได้ต่างกัน 200 ถึง 300% นอกจากนั้นสิ่งสำคัญที่ได้คือ ความเข้าใจ กลไกการเกิดสัณฐานที่เกิดขึ้นเมื่อผ่านขั้นตอนต่างๆ ทั้งนี้เนื่องจากในการผลิตผลิตภัณฑ์จากพอลิเมอร์ จะประกอบด้วย 2-3 ขั้นตอนที่มีการหลอมพอลิเมอร์ ดังนั้นจึงควรเข้าใจสัณฐานที่เกิดขึ้นในแต่ละขั้น และ สมบัติของผลิตภัณฑ์

คำหลัก: พอลิโอลิฟิน การขึ้นรูปวัสดุ สัณฐาน ความเหนียว

#### Abstract

Project Code:

BRG43-8-0012

Project title:

'Phase Behaviour of Polyolefin Blends under Melt Flow'.

Investigator:

Richard A. Venables

Tel.:

246-1358-74 Ext. 1309

Fax:

2477050

Email:

frrav@mahidol.ac.th

Project Period:

August 2000 to July 2003

Keywords:

polyolefin, processing, morphology, toughness

#### Objectives:

Characterisation of the solid state morphology in the linear polyethylene / ethylene- $\alpha$ -olefin copolymer blend that exhibits liquid-liquid phase separation, over the practical range of processing conditions used in fabrication, and comparison with the corresponding quiescent conditions.

Detailed investigation of processing - morphology relationships, physical characterisation, and physical property determination.

Microstructure - mechanical deformation analysis of selected, novel, liquid-liquid phase separation morphologies and immiscible blend morphologies through a fracture mechanics approach.

Ultimately, it is hoped that processing-morphology-property relations will be well established for this system, leading to the preparation of compounds with optimised that possess enhanced physical properties.

#### Method

To investigate the effects of thermomechanical history upon morphology evolution, samples were prepared with a well-defined history through solution blending followed by shearing at a range of temperatures. The morphology changes during subsequent annealing in the melt-state

were followed through quenching the samples from the melt and observing sections or prepared surfaces through microscopy.

#### Results and Discussion:

The thermomechanical history of polyolefin blends has a pronounced effect upon the morphology development, and therefore the physical properties of the materials. The effects of temperature and shear history differ depending upon the inherent mutual compatibility of the constituent polymers.

In systems that were deemed partially miscible, such as the polyethylene / poly(ethylene-co-1-octene) blend, melt flow resulted in the formation of a fine length-scale morphology comprising intertwined polyethylene lamellae and poly(ethylene-co-1-octene) domains. The morphology resulted from the concurrent liquid-liquid and solid-liquid phase separation that occurred upon cessation of flow and cooling.

In the partially miscible systems, shearing was found to affect the superposition of time and temperature upon the coarsening process that was observed for samples prepared without shearing. Shearing two-phase melts at 1 s-1 led to coarsening of the domain morphology at an accelerated rate in comparison with unsheared samples and those sheared at 50 s<sup>-1</sup>. In all cases, conditioning of samples at elevated temperature resulted in reduced coarsening during subsequent annealing. Moreover, the influence of elevated temperature was enhanced through intensive shearing during injection moulding. The short time spent at the elevated temperature has a critical effect upon the morphology that forms in subsequent operations. This effect was not a consequence of changes in melt viscosity, as evidenced by the non-superimposition of the results data when the superposition of time and temperature was assumed. The complex, multilayered phase morphology produced in the solid state during moulding, was the product of the partial miscibility in the melt state and the phase separation that takes place upon cooling and crystallisation. The resultant morphology has a marked bearing upon the toughness of the material under impact conditions at sub-ambient temperature. Coarser morphologies that are a consequence of higher elastomers contents and less compatibility of the blend components at lower temperature result in greater impact toughness at sub-ambient temperature.

In the isotactic polypropylene and isotactic poly(propylene-co-ethylene) systems that exhibited poorer compatibility than the polyethylene formulations, the impact properties were critically dependent upon the injection moulding conditions, with decreases in toughness associated with increased elastomer domain sizes at higher moulding temperatures. For the PE that exhibited pronounced miscibility in the melt-state, differences in the processing conditions had a relatively minor influence upon impact toughness.

The presence of the branched copolymer affected the fracture of PE differently depending upon the state of the test specimens. For crack propagation in the TD, the orientation of the PE dominated the fracture process and hence the presence of EOC had little effect. For crack propagation in the MD, the branched copolymer increased the non-essential work of fracture, but had little effect upon the essential work of fracture.

#### Conclusions:

It has been shown that the processing history has a pronounced effect upon the morphology development of polyolefin blends. The effect of shearing and temperature have a critical effect upon the morphology that forms through subsequent processes, in some cases resulting in a 200 to 300 % difference in measured toughness. Moreover, the key findings are that it is vital to understand the mechanism of morphology development since this has an important effect upon the morphology that is subsequently produced. This has particular relevance in polymer processing because polymer materials usually experience two to three stages of melt processing in the production of a finished article. Each step of the processing then must be considered to understand the morphology and properties of the finished article.

# FINAL REPORT

FACULTY OF SCIENCE, MAHIDOL UNIVERSITY

 $1^{\text{ST}}$  August  $2000 - 31^{\text{ST}}$  July 2003

# Phase Behaviour of Polyolefin Blends Under Melt Flow

BY

Richard A. Venables

#### Final Report

1. Project title: 'Phase Behaviour of Polyolefin Blends under Melt Flow'.

2. Researcher: Name:

Richard A. Venables

Qualification:

Ph.D. (Polymer Materials Science)

Position:

Foreign lecturer, Faculty of Science, Mahidol University.

Tel.:

246-1358-74 Ext. 1309

Fax:

2477050

Email:

frrav@mahidol.ac.th

3. Research branch: Polymer science

#### 4. PROPOSAL BACKGROUND AND OBJECTIVES

Polyolefins, such as polyethylene (PE), polypropylene (PP), and ethylene / α-olefin copolymers, constitute the most extensive group of industrially important polymers; moreover, the manufacture and conversion of polyolefins is by far the largest sector of the Thai polymer industry. Polyolefins may be blended together to give a wide range of materials from tough plastics to elastomers. Their use is expanding due to their low cost and ease of processing, in particular into applications where the incumbent is poly(vinyl chloride), partly because of the environmental hazards associated with the latter. The end-use properties of polyolefin blends depend strongly upon the phase morphology of the solid state. Blend morphology is determined principally by the thermodynamics of interaction between polymer molecules with differing types and quantities of chain-branches that control liquid-liquid and solid-liquid phase separation.

Whilst phase separation in polyolefin blends in the melt-state has been suspected, and known in some cases, recent work on model systems has increased the basic understanding of the phenomenon [Crist and Hill, 1997; Weimann et al., 1997]. Mechanical fracture studies, in combination with phase morphology characterisation, have begun to reveal how phase separation in the liquid state has a pronounced effect upon the solid state properties [Rhee and Crist, 1994]. These studies were carried out upon statically annealed samples, and hence the phase morphologies differ from those found in processed materials where the polymers are subjected to melt flow followed by rapid cooling. Phase morphology is greatly affected by melt flow, and hence it is necessary to extend these basic studies to the understanding of phase morphologyprocessing relationships such that materials with controlled morphologies may be obtained under realistic processing conditions.

The thought that melt flow affects phase behaviour thermodynamically does not seem to be widely appreciated, rather it has been considered that only the thermodynamic quantities associated with the polymer architecture, such as the presence of specific interactions and combinatorial entropy, are important. This is illustrated by a quote from the widely cited text 'Polymer-Polymer Miscibility' by Olabisi et al. [1979]:

".... the driving forces for the transition from the one-phase (miscible) to the two-phase (immiscible) state are thermodynamic in origin and do not depend, for example, on the extent or intensity of mixing."

The experimental work of Chen et al. [1995], concerning polystyrene / poly(vinyl methyl ether) blends, and the theoretical analysis of Horst and Wolf [1997], however, has shown that melt flow does contribute to the thermodynamics of mixing, most importantly through the contribution of stored elastic energy to the free energy of mixing. Our own recent studies, after collaboration with Prof. Takashi Inoue's group at the Tokyo Institute of Technology (TIT) in Japan, revealed that a linear polyethylene / elastomeric α-olefin copolymer blend exhibited extensive miscibility under melt-flow conditions and was essentially immiscible in the solid state. This was inferred from transmission electron microscopy results that revealed phase morphologies associated with liquid-liquid phase separation via the spinodal decomposition mechanism; thermal analysis confirmed that phase separation was complete in the solid state. Reports by Japanese polyolefin manufacturers have described similar effects in polypropylenebased blends [Inoue, 1998]; moreover, it has been suggested that these compounds exhibit enhanced properties over commercial blends possessing dispersed phase morphologies. The results show that flow contributes significantly to the thermodynamics of phase mixing. Additionally, Inoue [1998] has shown that even very low levels of flow induced miscibility may have significant effects upon end use properties.

Flow enhanced miscibility in polyolefin blends may prove to be an important mechanism to obtain novel morphologies and enhanced performance from these materials. Thus, a fuller understanding of this phenomenon and its effects under realistic processing conditions is needed. With this goal, a detailed study of the melt-flow / phase separation / morphology / property relationships was undertaken. It is envisaged that the work will elucidate the relationship between basic polymer architecture via melt processing to the final phase morphology in the solid state, and ultimately to the physical properties of the material. The insight gained is expected to aid in the development of new polyolefin blends with controlled morphologies and enhanced properties.

#### REFERENCES

Chen, Z. J., Wu, R. J., Shaw, M. T., Weiss, R. A., Fernandez, M. I., and Higgins, J. S., *Polym. Eng. Sci.*, (1995), 35(7), 92.

Crist, B. and Hill, M. J., Polymer, (1997), 35, 2329.

Dupont-Dow Elastomers, Product EG8150 data sheet, August (1996).

Hashemi, S., and Williams, J. G., Polym. Eng. Sci., (1986), 26(11), 760.

Hill, M. J., Barham, P. J., and Keller, A., Polymer, (1992), 33, 2530.

Hill, M. J. and Barham, P. J., Polymer, (1995), 36, 3369.

Hindawi, I. A., Higgins, J. S., and Weiss, R. A., Polymer, (1992), 33, 2522.

Horst, R. and Wolf, B. A., Polymer, (1997), 38(18), 4697.

Inoue, T., Special seminar presentation at Mahidol University, Thailand, Dec. (1998).

Kammer, H. W., Kummerlowe, C., Kressler, J., and Melior, J. P., Polymer, (1991), 32, 1488.

Katsaros, J. D., Malone, M. F., and Winter, H. H., Polym. Eng. Sci., (1989), 29, 1434.

Lee, C. H., Saito, H., and Inoue, T., Macromolecules, (1995), 28, 8096.

Mills, N. J. in, 'Plastics: Microstructure and Engineering Applications', 2nd Ed., Edward Arnold, London (1993)

Olabisi, O., Robeson, L. M., and Shaw, M. T., in Polymer-Polymer Miscibility', Academic Press, New York, (1979).

Otsuka, N., Yang, Y., Saito, H., Inoue, T., and Takemura, Y., Polymer, (1998), 39, 1533.

Puig, C. C., Hill, M. J., and Odell, J. A., Polymer, (1993), 34, 3402.

Rhee, J. and Crist, B., J. Polym. Sci.: Part B Polym. Phys., (1994), 32, 159

Saleemi, A. S. and Nairn, J. A., Polym. Eng. Sci., (1990), 30(4), 211.

Sano, H., Usami, T., and Nakagawa, H., Polymer, (1986), 27, 1497.

Takagi, S., Saito, H., Chiba, Chiba, T., Inoue, T., and Takemura, Y., Polymer, (1998), 39, 1643.

Weimann, P. A., et al., Macromolecules, (1997), 30(12), 3650.

Wu, J. and Mai, Y. W., Polym. Eng. Sci., (1996), 36(18), 2275.

Yamaguchi, M., Nitta, K., Miyata, H., and Masuda, T., J. Appl. Polym. Sci., (1997), 63, 467.

#### Outline of Report

This final report is presented as sections as the work has been published or is in preparation for publication. In part one, preliminary investigation into the mechanism of morphology is discussed. These results were published in the following journal:

Tabtiang T, Parchana B, Venables RA, Inoue T. 'Melt Flow Induced Phase Morphologies of a High-Density Polyethylene/Poly(ethylene-co-1-octene) blend'. J. Polym. Sci.: Part B: Polym. Phys., 39(3), (2001)

Part two contains a more detailed investigation of the effects of temperature and shear rate under controlled shear strain using well defined conditions in a cone-and-plate rheometer. Moreover, the effect of shear and thermal history upon subsequent morphology evolution is addressed. In part three, the influence of real processing conditions in an injection moulder upon the morphology and impact toughness of the blend systems is described. Results from these experiments have been published in the following journal:

Tabtiang T, Parchana B, Venables RA, 'The relationship between processing history and the morphology of injection moulded toughened polyolefins'. **Polym.-Plast. Technol. Eng.**, 40(4), pp.423-436 (2001)

Part four centres upon the effects of thermal history upon the morphology and toughness of the melt-processed blends. Part five is a detailed investigation of the influence of melt-flow induced orientation upon the plane stress fracture of the blend systems in which the mechanism of the influence of the two-phase morphology upon toughness is revealed.

## Contents

Results Part 1: Melt flow induced phase morphologies of a hig	h-density polyethylene /
poly(ethylene-co-1-octene) blend	p 1
Experimental	p 3
Results and discussion	p 4
Solution blends	p 4
Melt flow	p 5
Flow induced morphology	p 8
Lamella morphology	p 14
Conclusions	p 14
Results Part 2: Effect of thermomechanical history upon the co	parsening of morphology in
Experimental	р 18
•	
Results and discussion	p 19
Results and discussion  Effect of temperature	p 19 p 22
Effect of temperature	_
	p 22
Effect of temperature  Melt extrusion and injection moulded compounds	p 22 p 23 p 26
Effect of temperature  Melt extrusion and injection moulded compounds  Conclusions   Results Part 3: The relationship between processing history and	p 22 p 23 p 26
Effect of temperature  Melt extrusion and injection moulded compounds  Conclusions   Results Part 3: The relationship between processing history and moulded toughened polyolefins	p 22 p 23 p 26 
Effect of temperature  Melt extrusion and injection moulded compounds  Conclusions  Results Part 3: The relationship between processing history and moulded toughened polyolefins  Experimental	p 22 p 23 p 26 
Effect of temperature  Melt extrusion and injection moulded compounds  Conclusions  Results Part 3: The relationship between processing history and moulded toughened polyolefins  Experimental  Results and discussion	p 22 p 23 p 26 the morphology of injection p 29 p 30 p 32
Effect of temperature  Melt extrusion and injection moulded compounds  Conclusions  Results Part 3: The relationship between processing history and moulded toughened polyolefins  Experimental  Results and discussion  Isotactic polypropylene homopolymer formulations	p 22 p 23 p 26 the morphology of injection p 29 p 30 p 32 p 32

Results Part 4: Upon the morphology and toughness of a partially miso	tible high-density
polyethylene / poly(ethylene-co-1-octene) blend	p 42
Experimental	p 43
Results and discussion	p 44
Melt-state phase behaviour	P 44
Correlation of phase morphology with impact properties	p 50
Conclusions	p 54
Results Part 5: Plane stress fracture toughness of partially miscible high poly(ethylene-co-α-olefin) blends	n-density polyethylene , p 56
Experimental	р 57
Results and discussion	p 58
Orientation	<sub>P</sub> 59
Fracture studies	p 63
Conclusions	p 67
Final Conclusions	p 68

#### Results Part 1

# Melt flow induced phase morphologies of a high-density polyethylene / poly(ethylene-co-1-octene) blend

#### From the paper:

Tabtiang T, Parchana B, Venables RA, Inoue T. 'Melt Flow Induced Phase Morphologies of a High-Density Polyethylene/Poly(ethylene-co-1-octene) blend'. J. Polym. Sci.: Part B: Polym. Phys., 39(3), (2001)

#### Abstract

A blend of high-density polyethylene and an elastomeric poly(ethylene-co-1-octene) resin, containing 7 mol% of octene and long chain branching, was phase separated in the melt under quiescent conditions. After melt flow, the blend had fine globular or interconnected phase morphologies that were interpreted as originating from the various stages of coarsening after liquid-liquid phase separation through spinodal decomposition. It was inferred that the miscibility of the blend was enhanced under melt flow. Upon cessation of flow, concurrent liquid-liquid and solid-liquid phase separation took place, resulting in the formation of an interpenetrating morphology comprising amorphous polyethylene, copolymer, and crystalline polyethylene.

#### INTRODUCTION

The miscibilities of polyolefin blends are strongly affected by the extents of short and long chain branching in each polymer. Short chain branching is principally controlled by the types and quantities of the comonomers present. For example, propylene confers methyl, butene provides ethyl, and octene gives hexyl branches. A number of studies have described the partial miscibility of polyolefin blends, containing polymers with different branch levels, upon annealing under quiescent conditions. 1-2 In some instances, olefinic copolymers have been shown to exhibit partial miscibility with polypropylene due to the entropic repulsion created in the copolymer, caused by the dissimilarity of the co-monomers. 3-4.5 Melt processing profoundly affects the morphology of polymer blends, particularly when the polymers approach the limits of miscibility. At higher shear rates, flow enhanced miscibility has been observed, whilst demixing has also been observed at lower shear rates. These phenomena have been reported for the polystyrene / poly(vinyl methyl ether)<sup>7</sup> and polycarbonate / poly(styrene-co-acrylonitrile) systems. More recently, flow

enhanced miscibility has been observed in polyolefin blends under injection moulding conditions.9 Theories explaining these experimental data include the additive effect of melt elasticity to the free energy of mixing,10 changes in the specific interaction contacts, where relevant, and the alteration of the entropy of mixing.7 In most of the previous studies light scattering was used to follow changes in the cloud-point of blends under quiescent and shear flow conditions. 6,8 Several studies have reported upon the morphologies resulting from the meltprocessing of partially miscible blends. Okamoto et al.8 showed highly interconnected morphologies involving both phases in injection moulded blends of polycarbonate with poly(styrene-co-acrylonitrile) that possessed regular domain spacing. It was inferred that this was the hallmark of spinodal decomposition; dissolution of the blend components was reported at the barrel temperature of 260°C that was 37°C above the lower critical solution temperature at 223°C. Upon cessation of flow, phase separation took place. Sano et al.9 reported upon the morphologies in the skin region of injection moulded polypropylene / high-density polyethylene (60 / 40 w/w) blends, prepared at 240°C. In these samples, a regularly phase-separated structure comprising stripes with a periodic distance of around 0.15 µm was observed through transmission electron microscopy of ruthenium tetraoxide stained sections. In the micrographs, the bright areas consisted of crosshatched polypropylene lamellae whilst the darker areas comprised polyethylene lamellae of 10 nm thickness. It was inferred that this morphology was the result of depression of the upper critical solution temperature and / or the elevation of the lower critical solution temperature of the immiscible blend under the extreme flow conditions of up to 20,000 s<sup>-1</sup> found in the injection moulder. Whilst increases in the lower critical solution temperatures of around 50°C have been measured through light scattering studies,8 the results of Sano<sup>9</sup> suggest that greater changes may be obtained for polyolefin blends. The direct study of polyolefin blends through light scattering is limited, however, due to the similarity of the refractive indexes of the constituent polymers. Indirect studies through microscopy of quenched samples may offer an alternative route to investigate polyolefin systems.

In terms of volume of production, blends containing polyethylenes may be viewed as the most important commercial group. Commercial linear-low density polyethylenes are heterogeneous mixtures of lightly branched and highly branched copolymers of ethylene with  $\alpha$ -olefins, most often 1-butene and 1-octene. Phase separation in these materials under quiescent conditions in the melt-state has been reported.<sup>11</sup> The morphologies in the solid state, and hence properties, especially toughness, may be affected by the mixing and phase separation during processing. To investigate these phenomena under processing conditions, the work presented herein was carried out. In this report, the solid state morphology of a high-density polyethylene (HDPE) / poly(ethylene-co-1-octene) copolymer (EOC) blend is presented and some inferences concerning the scenario of phase behaviour in the melt state under flow are drawn.

#### EXPERIMENTAL

The HDPE used from Thai Polyethylene Co., Ltd., Thailand, had a melt flow index of 18 g/10min. The EOC, manufactured by Dow-Dupont Elastomers using a single site catalyst, had a melt flow index of 0.5 g/10min, melting point ≈ 50°C; it contained 7 mol% of octene and long chain branching. 12 Further details of these resin are documented in table 1. HDPE / EOC blends (72:28 wt%) were prepared either through melt blending using a Prism 16 mm twin screw extruder, employing a barrel temperature of 180°C and screw speed of 175 rpm, or through solvent blending. In the latter case, the resins were dissolved in boiling toluene under nitrogen and then precipitated by pouring into excess methanol. The BS 2782: Part 3, method 320A tensile specimens were prepared from the melt-blends using a Dr Boy 22S injection moulder, with barrel temperatures of 170 or 230°C; the screw speed was 100 min<sup>-1</sup>, the back pressure zero, and the cycle time was approximately 30 s. Selected mouldings and the solution blends were annealed in an oil bath, after wrapping in aluminium foil, for 15 min and 6 hr, respectively; the temperatures used were 170 and 230°C. Specimens, ≈ 15 µm in thickness, for dynamic mechanical analysis (DMA) were sectioned from the skins of the injection mouldings using a microtome. Analyses were carried out in tensile mode with a frequency of 10 Hz and heating rate of 5°C/min using a DMTA mkII thermal analyser from Polymer Laboratories. Differential scanning calorimeter (DSC) data were obtained with a Perkin Elmer DSC7 instrument: specimens (10 mg ± 0.1 mg) were cut from the central core of the mouldings and dipped in silicone oil to ensure rapid heat transfer to the specimens. Fusion endotherms were obtained at a heating rate of 30°C/min, to limit annealing during heating, under a nitrogen atmosphere. Transmission electron micrographs (TEM) were obtained from material at the skin and cores of the mouldings. The samples were flattened using an RMC Ultramicrotome at -100°C and then stained in sealed tubes above a RuO4 solution at 60°C for 1 h. The staining procedure was repeated three times using fresh reagent. Finally, sections of around 70 nm thickness were obtained from the stained samples through ultramicrotomy at room temperature. Sections were floated onto copper grids and were observed using an Hitachi H-300 microscope. Light micrographs were obtained of microtomed sections taken from the annealed solution blends using a Nikon E400 transmitted light microscope. Surfaces that were flattened using the ultramicrotome at -100°C were etched through immersion in permanganic acid for 24 h at 30°C. coated with platinum-palladium alloy, and viewed using an Hitachi S-2360N scanning electron microscope to obtain the number of spherulites per unit area in the cross-section. Rheological

data were collected using a Rosand capillary rheometer and a Haake RT20 parallel plate rheometer. Bagley and Rabinowitsch corrections were applied to the capillary rheometer data.

#### RESULTS AND DISCUSSION

#### Solution blends

Figure 1.1 shows light micrographs of the solution blends after annealing at 170 and 230°C for 6 hr under quiescent conditions. At both temperatures, distinct, large phase domains are visible. Banded spherulites are seen in one phase identifying it as being HDPE rich.

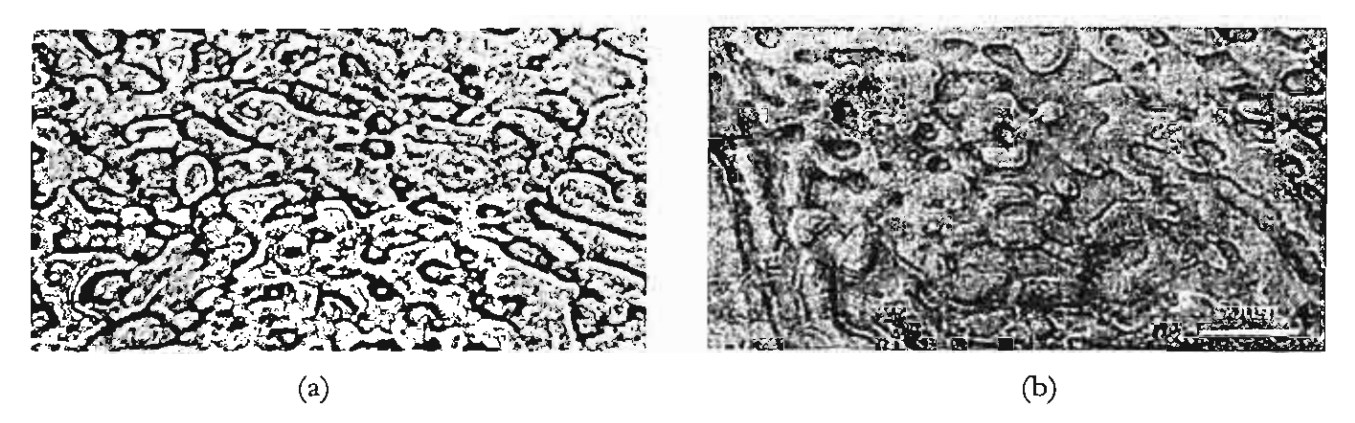


Figure 1.1 Light micrographs of solution blends after annealing at (a) 170°C and (b) 230°C for 6 h

Einstein's diffusion equation relates diffusion distance, x, to the diffusion rate, Dapp, and the time for diffusion, t:  $\overline{x^2} = 2D_{app}t$ . If  $D_{app}$  is 1.1 x  $10^{-10}$  cm<sup>2</sup>s<sup>-1</sup>, then x = 0.3  $\mu$ m for a 5 s diffusion time. Given the rapid quenching, within 5 s, after annealing the morphology is too coarse for it to result from phase separation during cooling, and hence it is inferred that the melt was biphasic. Direct observation of phase separation in the melt was not achieved, however, due to the closeness of the refractive indexes of the EOC and HDPE melts. In the solid state, the difference in density between the crystalline HDPE and the amorphous EOC provides contrast between the two phases. The area fraction of the EOC rich phase is greater than that expected from the 28 wt%, or 30 vol% at 25°C, EOC composition of the blend. Moreover, there is connectivity between the phase domains, rather than discretely dispersed droplets. A probable explanation is that a fraction of the HDPE dissolves into the EOC phase thereby increasing its effective volume fraction resulting in droplet coalescence, and hence domain connectivity. These observations suggest some limited miscibility in the melt at both 170 and 230°C. The extensive branching in the EOC precludes its co-crystallisation with the HDPE, and therefore solid-liquid phase separation will occur as the HDPE crystallises, leading to heterogeneity within the phase domains observed in Figure 1.1.

#### Melt flow

An estimate of the flow history in the injection moulder was obtained through the following analysis. The power dissipated per unit volume during plasticisation, P, was taken as:16

$$_{2}=\eta *(\dot{\gamma}_{c})^{2},$$

where  $\eta^*$  is the complex viscosity at angular frequency,  $\omega$ . It was assumed that  $\omega = \dot{\gamma}_c$ , i.e. the steady shear rate in the channel of the screw in the metering zone.<sup>17</sup>

$$\dot{\gamma}_c = \pi (D - 2h) N/h \,,$$

where D is the internal barrel diameter (24 mm), N the screw speed (100 min<sup>-1</sup>), and h the screw channel depth (2 mm); thus,  $\dot{\gamma}_c = 52 \text{ s}^{-1}$ . For the blend,  $\eta^* = 1,296$  and 585 Pa.s at 170 and 230°C, respectively. Specific mechanical energy input during plasticisation,  $S_c$ , was calculated  $S_e = Pt_p$ , where  $t_p$  is the plasticisation time (5 s);  $S_e = 17.5 \text{ MJm}^{-3}$  at 170°C and  $S_e = 7.9 \text{ MJm}^{-3}$  at 230°C. The shear rate at the wall of the nozzle,  $\dot{\gamma}_N$ , was estimated from 18

$$\dot{\gamma}_N = \left(4Q/\pi r^3\right)(3n+1)/4n\,,$$

where  $n = d \lg \tau / d \lg \dot{\gamma}$ ,  $Q = v_{T,P} m / t_1$ , Q is the melt injection rate, m the shot weight (15 g),  $v_{T,P}$  is the specific volume of the melt at temperature, T, and injection pressure, P (3.4 MPa),  $t_1$  is the injection time (2 s), r is the radius of the nozzle orifice (1.25 mm),  $\tau$  is the shear stress at the wall, and n is the non-Newtonian exponent. Both at 230°C and 170°C,  $\dot{\gamma}_N \approx 6,500 \text{ s}^{-1}$ , assuming specific melt volumes of 1.27 and 1.33 cm<sup>3</sup>g<sup>-1</sup> for melts at 170°C and 230°C, respectively, under 3.4 MPa of pressure.<sup>19</sup> A description of the cooling process in the injection mouldings may be obtained using the Fourier equation for non-steady heat flow in one dimension:<sup>20</sup>

$$\partial T/\partial t = \alpha (\partial^2 T/\partial x^2),$$

where T is the temperature, t is time,  $\alpha$  is the thermal diffusivity, and x is the distance between the part of the moulding in question and the mould surface. The thermal diffusivity is related to k, the thermal conductivity,  $\rho$ , the density, and  $C_P$ , the specific heat capacity:  $\alpha = k/\rho C_P$ ; data are given in table 1.

Table 1. Polymer characteristics

Parameter		Polymer			Blend	
		PE	P1O	EOC	(70/30 v <sub>PE</sub> /v <sub>EOC</sub> )	
C <sub>∞</sub>		7.00 <sup>a</sup>	9.10a	7.53 <sup>b</sup>	-	
ь	(nm)	0.815	0.929	0.845	-	
$M_w$	(gmol-1)	45,000	-	162,700	-	
$M_0$	(gmol·1)	28.054	112.216	49.095	-	
n		3,207	-	6,627	-	
n <sub>s</sub>		802	-	1,657	-	
$R_g$	(nm)	9.4	-	14.0	12.1	
r	(nm)	23.1	-	34.4	29.6	
L	(nm)	-	-	-	17.1	
$ m V_{25^{\circ}C}$	$(cm^3mol^{-1})$	33.1°	130.8c	57.5	-	
ρ <sub>25°C</sub>	(gcm <sup>-3</sup> )	0.962 <sup>d</sup>	-	0.868 <sup>d</sup>	-	
α	$(m^2s^{-1}) \times 10^7$	1.57°	-	1.17°	1.46 <sup>r</sup>	
D <sub>170°C</sub>	$(cm^2s^{-1}) \times 10^{10}$	1.28	-	0.22	0.36	
D <sub>230°C</sub>	$(cm^2s^{-1}) \times 10^{10}$	2.82	-	0.71	1.10	

areference;13

If the cooling of the melt at the mould surface may be described by the one-sided heat conduction into a semi-infinite body and that  $\alpha$  is constant over the temperature change, an estimate of the cooling rate may be made. Two-sided heat transfer was used to describe cooling of the core. The dimensionless Fourier parameter,  $F_0$ , is calculated  $F_0 = \alpha t/x^2$ . In the core, x is half the moulding thickness (x = 3.2 mm / 2); in the skin region, x is the distance from the mould surface to where the TEM sections were obtained (0.1 mm). A plot of the temperature gradient,  $\Delta T$ , where

$$\Delta T = (T_{x,t} - T_{ms})/(T_0 - T_{ms})$$

bdata for EOC calculated from the copolymer composition weighted average of the values for PE and P1O;

creference;14

dtypical density at 25°C;

ereference, 15 assuming that  $\alpha$  for EOC is equal to that of LDPE;

fcalculated from the mass fraction weighted average of the values for PE and EOC.

against  $F_0$  for a flat sheet was used to find  $F_0$  at  $\Delta T$ , and hence the time to reach  $T_{x,t}$  may be found;<sup>21</sup>  $T_{ms}$  is the mould surface temperature (30°C),  $T_0$  is the initial melt temperature (230°C or 170°C),  $T_{x,t}$  is the temperature at x after time t.  $T_{x,t}$  was taken as the estimated temperature where the crystal growth rate of polyethylene is a maximum. This is<sup>22</sup> 5,000  $\mu$ mmin<sup>-1</sup> at 112°C, that is 30°C below the equilibrium melting point of 142°C. Thus,  $T_{x,t} = 112$ °C, and hence for a melt temperature of 230°C,  $\Delta T = 0.41$ ,  $F_0 = 0.46$ , and the time taken to reach 112°C is 8.1 s in the core and 0.03 s at the skin. For the 170°C melt temperature, the corresponding values are:  $\Delta T = 0.59$ ,  $F_0 = 0.31$ , and the cooling times in the core and skin are 5.4 and 0.02 s, respectively. The crystallisation process in the core was assumed to be zeroth order three-dimensional spherulite growth. The number of spherulite nuclei in the cross-section of the core,  $N_A$ , was 1.06 x 10<sup>-2</sup>  $\mu$ m<sup>-2</sup>. This value was determined by point counting the spherulite centres in the SEM micrographs of permanganic acid etched surfaces. The number average spherulite diameter in the cross-section,  $D_{nA}$ , was 10.6  $\mu$ m. The number average diameter in volume,  $D_{nV}$ , was:<sup>20</sup>

$$D_{nV} = (4/\pi)D_{nA}.$$

The number of spherulite nuclei per unit volume, Nv, was

$$N_V = N_A / D_{nV} ;$$

 $N_v = 7.9 \times 10^{-4} \ \mu m^{-3}$ . To reach a maximum random packing fraction at impingement of the spherulites,  $\phi_{max}$ , of  $\phi_{max} \approx 0.7$ , from:<sup>24</sup>

$$\phi_{\text{max}} = N_V \pi D_{nV}^3 / 6$$

at a spherulite growth rate of 83 µms<sup>-1</sup> the time taken was 0.07 s after 112°C was reached. The time taken for the melt to solidify is the sum of the cooling time and crystallisation time; at the end of this period, the morphology is effectively frozen-in. For the melt at 230°C, the solidification time was 8.2 s in the core and 0.10 s at the skin. The corresponding values for the 170°C melt were 5.5 and 0.09 s, respectively.

#### Flow induced morphology

Figure 1.2 displays TEM micrographs of the core regions of the as-moulded blends, prepared at 170°C and 230°C, together with images of the original HDPE resin processed under comparable conditions.

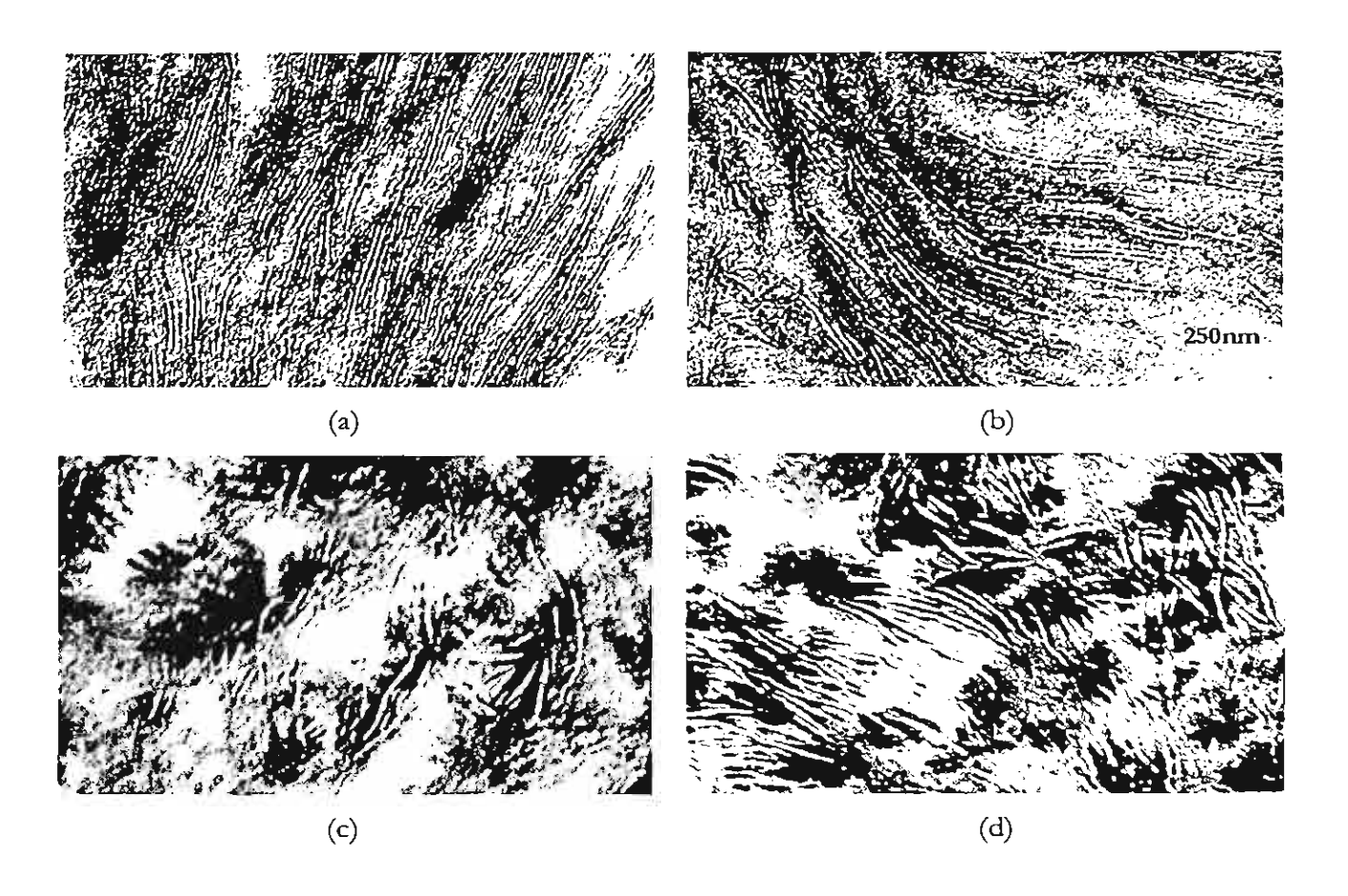


Figure 1.2 TEM micrographs of the as-moulded specimens in the core region, prepared at two temperatures: HDPE at (a) 170°C and (b) 230°C and the HDPE / EOC blend at (c) 170°C and (d) 230°C.

The near amorphous EOC constitutes the most heavily stained domains, whilst amorphous HDPE is more lightly stained; the HDPE lamellae are unstained. DMA traces of the HDPE resin, EOC, and the skin of a blend moulding prepared at 230°C are shown in Figure 1.3. The blend exhibits loss maxima at -115°C and -32°C that may be assigned to the glass transitions of HDPE and EOC, respectively. Whilst the T<sub>g</sub> of the original HDPE and the HDPE in the blends were essentially the same, for all injection moulded blends, T<sub>g</sub> of the EOC was 5 to 7°C higher than that of the original EOC, i.e. -37°C; moreover, the relaxation peaks were slightly broader. In some locations in the blend, the EOC is pinned between neighbouring HDPE lamellae and consequently this may hinder its mobility, giving rise to the slight increase in T<sub>g</sub> of the EOC. The peak broadening may result from the EOC being located both between the lamellae and in less confined domains that result in a distribution of local environments, each possessing different

relaxation characteristics. The solid state phase domains largely comprise pure amorphous HDPE, pure EOC, and crystalline HDPE.

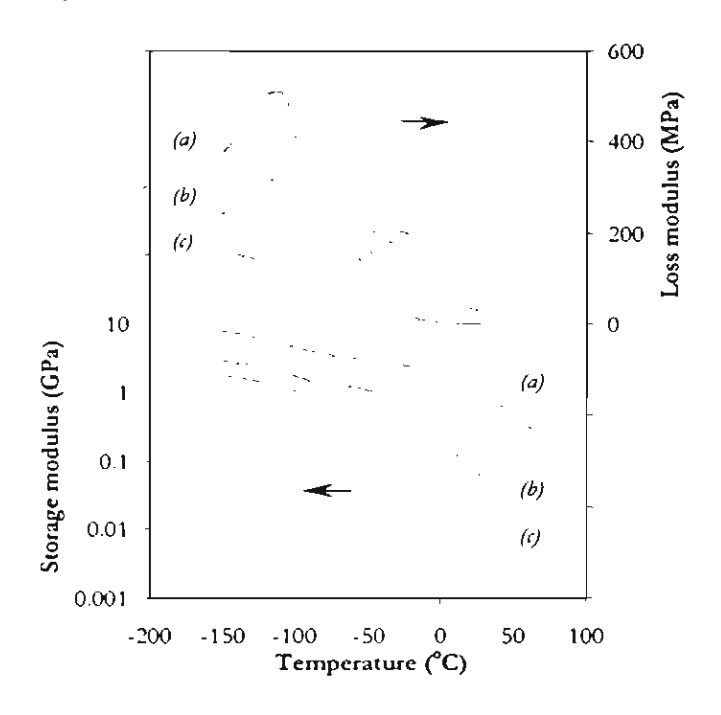


Figure 1.3 Typical DMA traces for (a) HDPE, (b) HDPE / EOC blend, and (c) EOC. The specimens were microtomed from the skins of the injection mouldings; the loss modulus curves of the blend and PE are offset from the EOC curve by +50 MPa for clarity.

In the injection-moulded blends, the EOC appears as an interconnected arrangement of globules that is intertwined with swathes of HDPE lamellae. The HDPE lamellae penetrate extensively into the EOC domains, indicating that crystals grew from, or into, a mixed phase containing both EOC and HDPE.



Figure 1.4 Overview of the EOC domain morphology in the core region of a blend moulded at 170°C.

The length-scale of the EOC phase domains is very fine, with an average periodic distance in the EOC-rich areas of 154 nm. This morphology is unlikely to result simply from the mechanical

work of dispersive mixing, since the dynamic equilibrium of droplet break-up and coalescence confers a lower mean particle size limit for physical dispersive mixing in polymer blends of around 0.5 µm, although smaller domain are possible in reactive systems. Thus, it is inferred that the fine morphology is the product of concurrent liquid-liquid and solid-liquid phase separation from a mixed, or partially mixed melt, and hence that the flow during injection moulding enhances the miscibility of the blend. Bi-continuous morphologies are evident in the image of the core of a moulding prepared at 170°C, displayed in Figure 1.4.

The effects of the local cooling conditions in the mould are illustrated by the differences in the skin and core morphologies of the blend moulded at 230°C, shown in Figure 1.5.

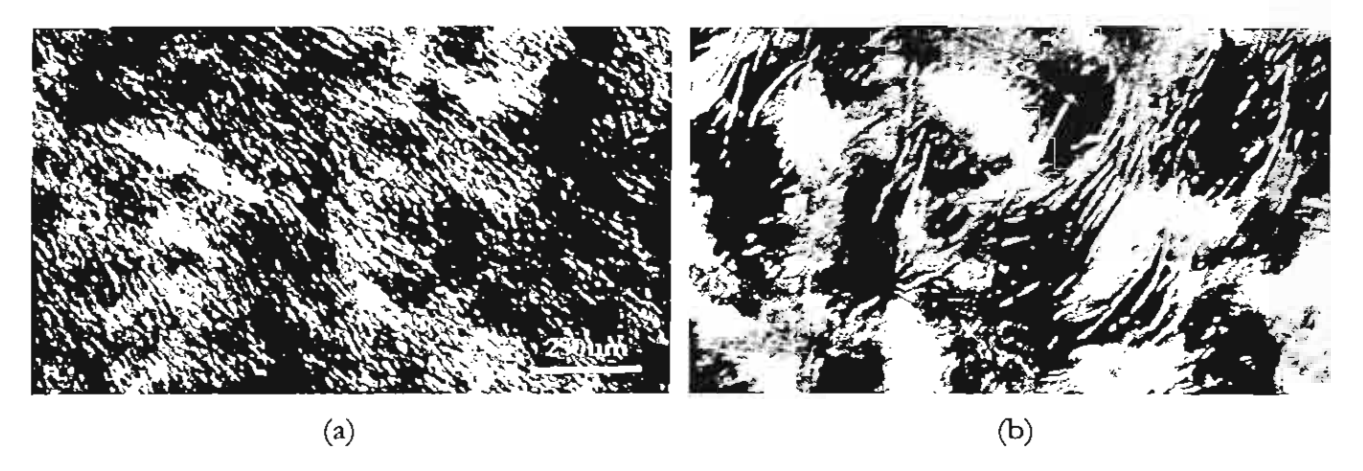


Figure 1.5 TEM micrographs of (a) skin and (b) core areas of a blend moulded at 230°C.

At the skin, the EOC is more evenly distributed, whilst in the core the EOC domains are larger and more distinct from the HDPE rich areas. Moreover, the HDPE lamellae are thinner and less well defined in the skin.

A description of the morphology evolution may be obtained through the following discussion. The statistical segment length, b, is given by

$$b = \left(C_{\infty} n L^2 / n_s\right)^{\frac{1}{2}},$$

where n is the number of backbone carbons,  $n = (2M_w/M_0) - 1$ , n, is the number of statistical segments, based upon a four carbon unit,  $n_s = (M_w/2M_0)$ ,  $M_w$  is the weight average molecular weight,  $M_0$  is the molecular weight of the polymer repeat unit, and L is the C-C bond length (0.154 nm), and  $C_\infty$  is the characteristic ratio.  $R_g$  and r are the root mean square radius of gyration and root mean square end-to-end distance of the polymer chain:<sup>25</sup>  $R_g = b(n_s/6)^{\frac{1}{2}}$  and

 $r = b(n_s)^{\frac{1}{2}}$  or  $r = 6^{\frac{1}{2}}R_g$ . These data are summarised in table 1; data for the ECO were calculated from the mole-fraction weighted averages of the experimental data obtained for PE and poly(1-octene) (P1O). The radius of gyration for a mixture of polymer 1 and 2, where polymer 1 is PE and polymer 2 is EOC, is given:<sup>26</sup>

$$R_{g} = \left(\frac{n_{s(1)}n_{s(2)}(\phi_{2}b_{1}^{2} + \phi_{1}b_{2}^{2})}{6(\phi_{1}n_{s(1)} + \phi_{2}n_{s(2)})}\right)^{L_{2}},$$

where  $\phi_1$  is the volume fraction of polymer j. The polymer-polymer interaction length, L, is determined  $L = r/3^{\frac{1}{2}}$ ; the kinetically favoured length-scale for demixing,  $\lambda_m$ , is related to the demixing temperature, T, and the temperature at the spinodal,  $T_s$ , from:<sup>27</sup>

$$\lambda_m/L = 2\pi (3|T - T_s|/T_s)^{-1/2}$$
.

The 70:30  $v_{PE}$ : $v_{EOC}$  blend was found to be two-phase in the quiescent melt at all temperatures investigated, that is in the range 150 to 350°C. Limited miscibility for EOC contents of 10 vol% and lower were found at 350°C. The critical point,  $\phi_2$ c is

$$\phi_2^c = (1 + (v_2 n_2 / v_1 n_1)^{1/2})^{-1} = 0.35,$$

where  $v_1$  is the monomer volume of component j. Extrapolation of the 'cloud-point curve' to  $\phi_2^c$  gave an approximate  $T_s$  of 400°C, the corresponding  $\lambda_m$  values for demixing at 230°C and 170°C would be 95 and 82 nm, respectively; that is  $\lambda_m$  decreases with increasing quench depth in a system with an upper critical solution temperature. The observed value of  $\lambda$  in the blend prepared at 230°C was 154 nm. The growth rate of fluctuations,  $R_{q(t)}$ , at scattering vector, q, is included in the following expression:

$$I_{q(t)} = I_{q(t=0)} \exp R_{q(t)}$$

where  $q_m = 2\pi/\lambda_m$  and  $I_{q(t)}$  is the Fourier component, or scattering intensity, at q and time, t. The maximum growth rate,  $R_m$ , is

$$R_m = q_m^2 D_{app} / 2.$$

The mutual diffusion coefficient, Dapp, is found:

$$D_{app} = \frac{D_1 D_2 \left( \phi_1 n_{s(1)} + \phi_2 n_{s(2)} \right)}{\phi_1 n_{s(1)} D_1 + \phi_2 n_{s(2)} D_2} f,$$

where  $D_i$  is the self-diffusion coefficient of polymer j,  $D_j = k_j M_{(j)}^{-2}$ , M is molecular weight, and f is a factor that describes the slowing of diffusion as the spinodal temperature is approached. In the specimens described herein, the quench is relatively deep; i.e.,  $|T_s - T| \ge 200^{\circ}C$ , and consequently no slowing is considered. The temperature dependence of  $D_i$  is

$$D_j/T = Ae^{-E_{D/T}/RT}.$$

For linear PE,<sup>28</sup> E<sub>D/T</sub> = 24 kJmol<sup>-1</sup> and k = 0.26 cm<sup>2</sup>g<sup>2</sup>mol<sup>-2</sup>s<sup>-1</sup>. These values are not known for EOC, thus values were estimated from the data of Bartels et al.<sup>29</sup> for poly(ethylene-co-1-butene). The calculated growth rates at 230 and 170°C are 23.9 and 10.6 s<sup>-1</sup>, respectively. The growth exponent is the product of R<sub>m</sub> and the time allowed for growth, t; in this case t was taken as the solidification time of the moulding. R<sub>m</sub>t at the skin and core for the melt at 230°C are 2.4 and 196, respectively; at 170°C the corresponding values are 1.0 and 58. The early stages are coarsening may be considered as  $R_m t \le 1.1$ .



Figure 1.6 Core region of a blend moulded at 230°C: (a) as-moulded and (b) after annealing at 230°C for 15 min.

Thus, the morphology observed in the core region may have coarsened beyond the early stage, and hence q decreases below  $q_m$ , and  $\lambda$  is greater than  $\lambda_m$ , whereas at the skin, the texture may be a consequence of the freezing-in of the early stage of phase separation.

Figure 1.6 shows the globular core morphology of the 230°C as-moulded melt-blend, alongside the same moulding after annealing at 230°C for 15 min. In the melt under quiescent conditions, the EOC domains coalesce and occlude some of the HDPE rich phase, suggesting that this fraction of the HDPE does not re-dissolve into the EOC under static conditions. Detail of the domains in the blend moulded at 170°C and annealed at 170°C for 15 min, are displayed in Figure 1.7. HDPE lamellae can be seen penetrating into the EOC domain, from which it is inferred that some HDPE was mixed with the EOC under quiescent conditions in the melt.

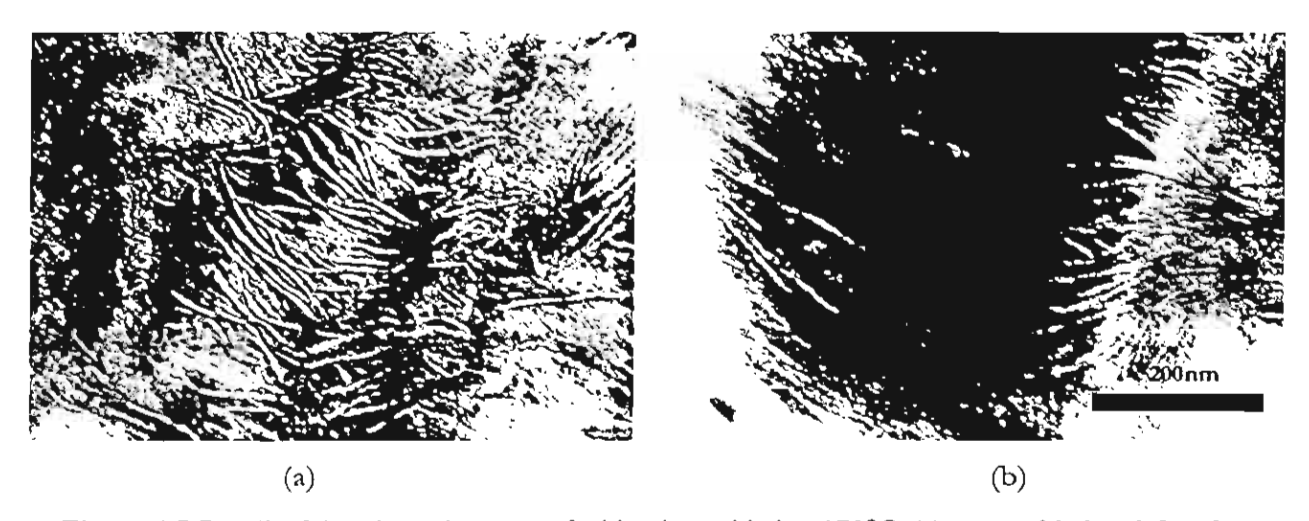


Figure 1.7 Detail of the phase domains of a blend moulded at 170°C: (a) as-moulded and (b) after annealing at 170°C for 15 min.

The extent of interpenetration is considerably less than that seen in the melt-blend, however, and hence it is concluded that the melt flow in the injection moulder drives the blend towards miscibility. The spinodal boundary, which may be an upper and / or lower critical solution temperature type, may be shifted due to the melt flow. Upon cessation of flow and cooling, phase separation occurred rapidly and was complete within the cooling stage of the moulding cycle. From the connectivity of the minor phase and the rapidity of the moulding cycle, phase separation is likely to have occurred through spinodal decomposition. Moreover, the shape and arrangement of the EOC domains are consistent with this mechanism. The length-scales of the observed morphologies are of the order of magnitude expected from phase separation, based upon estimates of the molecular dimensions.

#### LAMELLA MORPHOLOGY

In the moulded blends, the HDPE lamellae penetrate the EOC rich areas and extend into the HDPE rich phase. Moreover, the highly stained regions at the edges of the lamellae show strong contrast with the unstained crystalline material due to the concentration of the EOC at these locations. The extensive chain branching in the EOC precludes its incorporation into the HDPE lamellae, and consequently as the HDPE crystallises from the mixed phase the EOC collects at the edges of the lamellae. This is further evidence that the polymers were mixed in the melt. The presence of EOC between the HDPE lamellae results in a distribution of the long period values, ranging from around 18 nm in HDPE rich areas to 27 nm in EOC rich regions, although there is little change in the average lamella thickness between the blend and the original HDPE prepared at the same moulding temperature. This indicates that the melt was not homogeneous at the onset of crystallisation, with the more closely packed lamellae forming from HDPE rich regions and the thicker inter-lamellar regions the product of crystallisation from areas with higher EOC concentrations. As the melt cools from above 200°C through the spinodal boundary, liquid-liquid phase separation will begin and will continue unperturbed until HDPE crystallisation begins at temperatures below about 120°C. At this point, HDPE lamellae grow rapidly from both EOC rich and HDPE rich areas. With close inspection of the PE lamellae in the melt-blends, in Figure 1.2, it is evident that the lamellae are not as straight as those seen in the original HDPE mouldings, with some exhibiting an abrupt kink, whilst others have a more gentle wave conformation. This may be caused by the presence of EOC impurity in the HDPE melt during crystallisation. The overall crystallinity of the HDPE, as determined through DSC, was significantly affected neither by moulding temperature nor by liquid-liquid phase separation, since all determinations fell in the range 62.4 to 62.8%.

#### CONCLUSIONS

Melt flow during processing of the HDPE / EOC blend that is partial miscibility under quiescent conditions resulted in the formation of a fine length-scale morphology comprising intertwined HDPE lamellae and EOC domains. It may be inferred that the morphology resulted from the concurrent liquid-liquid and solid-liquid phase separation that occurred upon cessation of flow and cooling.

#### REFERENCES

- 1. Hill, M. J.; Barham, P. J. Polymer 1995, 36(17), 3369.
- 2. Hill, M. J.; Barham, P. J.; Keller, A. Polymer 1992, 33(12), 2530.
- 3. Otsuka, N.; Yang, Y.; Saito, H.; Inoue T.; Takemura, Y. Polymer 1998, 39(8-9), 1533.
- 4. Lee, C. H.; Saito, H.; Inoue, T. Macromolecules 1995, 28, 8096.
- 5. Yamaguchi, M.; Nitta, K.; Miyata, H.; Masuda, T. J Appl Polym Sci 1997, 63, 467.
- 6. Hindawi, I. A.; Higgins, J. S.; Weiss, R. A. Polymer 1992, 33(12), 2522.
- 7. Katsaros, J. D.; Malone, M. F.; Winter, H. H. Polym Eng Sci 1989, 29(20), 1434.
- 8. Okamoto, M; Shiomi, K; Inoue, T. Polymer 1995, 36(1), 87.
- 9. Sano, H.; Yui, H.; Inoue, T. Polymer 1998, 39(21), 5265.
- 10. Kammer, H. W.; Kummerlowe, C.; Kressler, J; Melior, J. P. Polymer 1991, 32(8), 1488.
- 11. van Ruiten, J.; Boode, J. W., Polymer 1992, 33(12), 2548.
- 12. Dupont-Dow Elastomers product EG8150 data sheet; August 1996.
- 13. Bicerano, J. In Prediction of polymer properties, Marcel Dekker: New York, 1993; Chapter 12, p 286.
- 14. Bicerano, J. In Prediction of polymer properties, Marcel Dekker: New York, 1993; Chapter 3, p 66.
- 15. Crawford, R. J. In Plastics Engineering: 2<sup>nd</sup> Edition, Pergamon Press: Oxford, 1987; Chapter 1, p 33.
- 16. Morton-Jones, D. H. In Polymer Processing; Chapman and Hall: London, 1989; p. 71.

- 17. Rauwendaal, C. In Polymer Extrusion: 2nd Edition; Hanser Publishers: Munich, 1990; Chapter 6, p 181.
- 18. Nielson, L. E. In Polymer rheology: Marcel Dekker: New York, 1977; Chapter 1, p 16.
- 19. Grulke, E. A. In Polymer process engineering; PTR Prentice Hall: New Jersey, 1994; Chapter 10, p 577.
- 20. Crawford, R. J. In Plastics Engineering: 2<sup>nd</sup> Edition; Pergamon Press: Oxford, 1987; Chapter 5, p 279.
- 21. Crawford, R. J. In Plastics Engineering: 2nd Edition; Pergamon Press: Oxford, 1987; Chapter 5, p 280.
- 22. Progelhof, R. C.; Throne, J. L. In Polymer Engineering Principles; Hanser Publishers: Munich; 1993, Chapter 2, p 129.
- 23. Dehoff, R. T. In Quantitative microscopy; McGraw-Hill: New York, 1968; Chapter 5, p 131.
- 24. Wypych, G. In Fillers; ChemTec Publishing: Canada, 1993; Chapter 4, p 143.
- 25. Gedde, U. W. In Polymer Physics; Chapman and Hall: London, 1995; Chapter 2, p 21.
- 26. Rhee, J.; Crist, B. Macromolecules 1991, 24, 5663.
- 27. Olabisi, O., Robeson, L. M.; Shaw, M. T. In Polymer-polymer miscibility; Academic Press: New York, 1979; Chapter 2, p 46.
- 28. Klein, J.; Fletcher, D.; Fetters, L. J. Faraday Symp Chem Soc 1983, 18, 159.
- 29. Bartels, C. R.; Crist, B.; Graessley, M. W. Macromolecules 1984, 17, 2702.

#### Results Part 2

# Effect of thermomechanical history upon the coarsening of morphology in polyethylene blends

#### Abstract

High-density polyethylene (PE) / poly(ethylene-co-1-octene) (EOC) blends, prepared through solution blending, were sheared under controlled conditions of temperature and shear rate in a cone-and-plate rheometer using steady flow. Samples were also prepared through melt blending and injection moulding at various temperatures. The evolution of the two-phase melt-state morphology was inferred through characterisation of samples that were annealed in the melt-state as a function of time and then rapidly quenched. At very low shear rates, of around 1 s<sup>-1</sup>, it was found that the coarsening rate was increased relative to the that of a sample prepared through solution blending that had experienced no melt flow. At higher shear rates, around 50 s<sup>-1</sup>, coarsening rates were slower than those found at the lower shear rate. Increased melt-processing temperature was found to decrease the subsequent coarsening rate under quiescent conditions. Samples that were injection moulded experienced the highest shear rates up to 10,000 s<sup>-1</sup>. Whilst differences in shear rate for high levels of specific energy dissipation produced insignificant differences in coarsening rate, increased processing temperature resulted in a reduced coarsening rate that was proportional to the processing temperature.

#### INTRODUCTION

Physical properties are affected by the solid-state morphology. The interactions of processing variables, such as temperature, shear rate, stress, shear strain, etc. affect the evolution of two-phase morphology in the melt state and therefore the morphology of the solid state. In this phase of the work, the effects of thermo-mechanical flow history upon subsequent morphology development were investigated. In earlier experiments, the direct influence of mechanical work has been characterised. However, plastics compounds are usually processed over several stages of heating and cooling so it is important to know the effects of the prior flow and thermal treatment upon the subsequent behaviour of the compounds. To this end, samples were sheared under controlled conditions of shear rate, shear stress, total shear strain, and temperature to produce morphologies that were prepared under well-defined conditions. To prepare samples with the intense shear and thermal histories experienced in real plastics

processing operations, samples were also compounded then injection moulded under various conditions.

#### **EXPERIMENTAL**

The PE had a melt flow index of 14 g/10min, weight average molecular weight,  $M_w$ , 48,000 g/mol, and nominal density 0.962 g/cc. The copolymer used, , had a melt flow index of 0.5 g/10min,  $M_w = 162,700$ ,  $M_w / M_n = 2$ , and density 0.868 g/cc; it contained 7 mol<sup>o</sup> o octene.

Solution blends, containing 20 wto of EOC, were prepared through dissolution of the resins in hot toluene followed by precipitation in methanol. The samples were then filtered and dried in air for one day followed by 3 hours under vacuum at 80°C. Samples were consolidated and pressed into disks of 20 mm diameter and 3 mm thickness.

Controlled shear experiments were carried out using a Haake RT20 cone-and-plate rheometer under steady flow conditions. The dimensions and geometry of this apparatus are illustrated in figure 2.1.

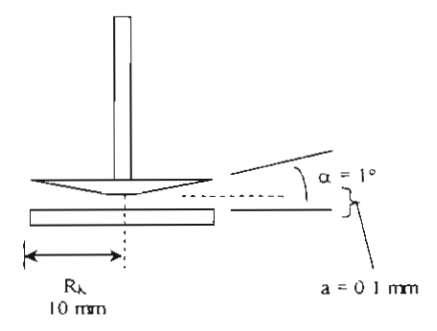


Figure 2.1 Cone and plate rheometer geometry; distance 'a' is the gap between the cone and the plate

Stress, \u03c4, was calculated:

$$\tau = AM_{\perp}$$

where  $M_4$  is the torque and A is geometry factor:

$$A = 3/2\pi R_K^3$$

where  $R_K$  is the cone radius. The shear rate,  $\dot{\gamma}$ , is determined:

$$\dot{\gamma} = \Omega/\alpha$$

where  $\alpha$  is the cone angle, accurately calibrated for each cone, and  $\Omega$  is the angular velocity that is calculated:

$$\Omega = 2\pi n/60$$

where n is the speed of cone rotation. The total deformation, v, is then:

$$\upsilon = \varphi/\alpha$$

in which  $\varphi$  is the torsion angle. Total strain,  $\overline{w}$ , is thus the following function:

$$\varpi = (\upsilon - \upsilon_0)/\upsilon_0$$

where  $\upsilon$  is the given strain and  $\upsilon_0$  is the initial deformation. Experiments were carried out by shearing each sample under continuous shear at a given shear rate and at constant total strain. The condition of  $\varpi = 300$  was arbitrarily chosen to give shearing times in the range of 6 to 300 s for samples sheared at 50 and 1 s<sup>-1</sup>, respectively. Temperatures of 170, 200, or 230°C were used. Rotation of the shaft was then halted and the cone and plate was separated. Sampling was subsequently achieved by removing the melt with a wooden rod and quenching the melt by plunging the sample into and ice / water mixture. Pieces of the quenched material were annealed for times between 5 and 30 minutes at 170, 200, or 230°C and then quenched.

Stubs for scanning electron microscope (SEM) observation were obtained using an RMT ultramicrotome. Surfaces were etched with permanganic acid reagent (1 % w/v) at room temperature for 18 hours and were viewed after vapour deposition of a platinum-palladium alloy.

#### **RESULTS AND DISCUSSION**

Figure 2.2 shows the dispersed phase dimensions for the solution blends annealed at 170, 200, or 230°C without shearing. Apparently, the data are clustered around a single curve. This shows the equivalence of the effects of time and temperature, that is a longer annealing time or higher temperature results in proportionally coarser morphologies. Higher temperature decreases melt viscosity and so coarser morphologies are attained for a given annealing time. Figure 2.3 shows the domain sizes of the samples that were sheared at 1 and 50 s<sup>-1</sup> plotted alongside the data for the un-sheared samples prepared at 170, 200, or 230°C. Domain sized increased approximately

linearly as a function of the cubed root of time, and hence the coarsening mechanism in each sample is consistent with the mechanism of Oswald ripening for spherical dispersed particles.

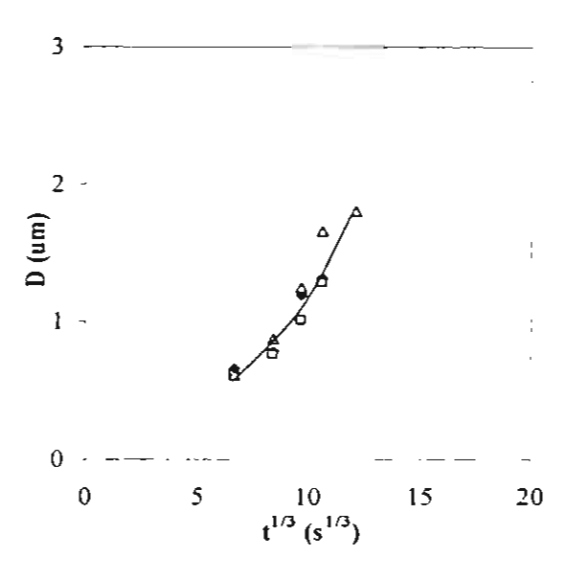
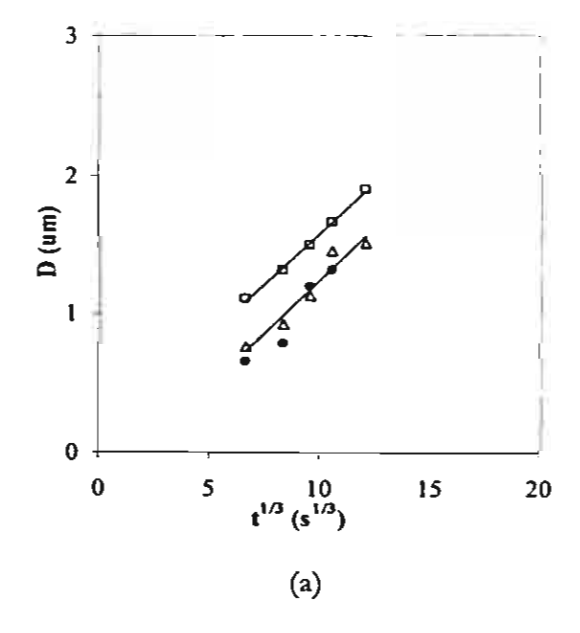
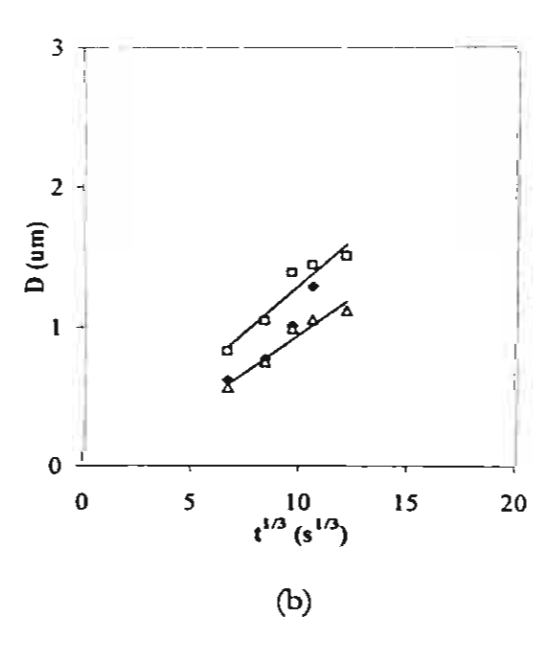


Figure 2.2 Etched domain diameter, D, versus annealing time, t, of solution blends annealed without shearing at (♠) 170, (□) 200, and (Δ) 230°C

Apparently, shearing at 1 s<sup>-1</sup> results in coarser morphology at every annealing time, in comparison with the unsheared melts and those sheared at 50 s<sup>-1</sup>. Unsheared melts and melts sheared at 50 s<sup>-1</sup> gave essentially equal results. This result may be affected by the time that the samples spent under shearing. The samples were prepared such that all the sheared materials experienced the same total strain of 300.





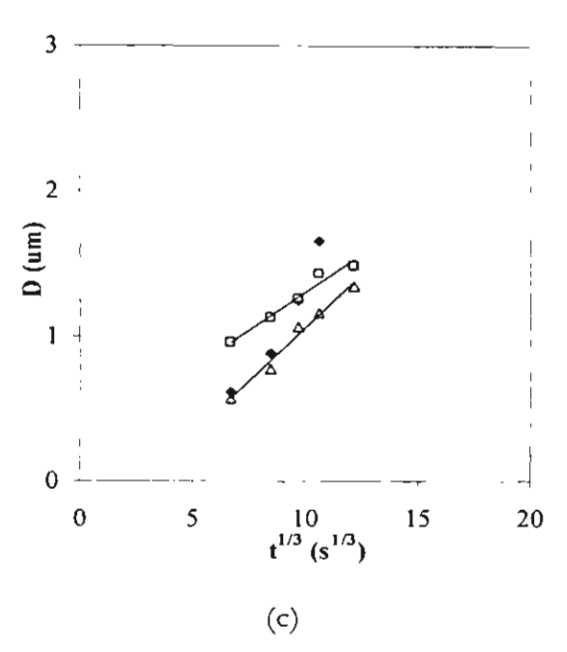


Figure 2.3 Etched domain, D, of morphology of solution blends versus annealing time, t, annealed at (a) 170°C, (b) 200°C, and (c) 230°C: ( $\spadesuit$ ) un-sheared and sheared at ( $\square$ ) 1 s<sup>-1</sup> and ( $\Delta$ ) 50 s<sup>-1</sup>.

Thus, the samples were necessarily sheared in the melt for different times such that the same total strain could be imposed. To account for this time difference, annealing times were corrected for the time spent under shear; thus, the following is defined:  $t^* = t + t_s$  where  $t^*$  is the corrected annealing time, t is the actual annealing time, and t, is the time spent under shear. The corrected annealing times,  $t^*$ , are plotted in figure 2.4.

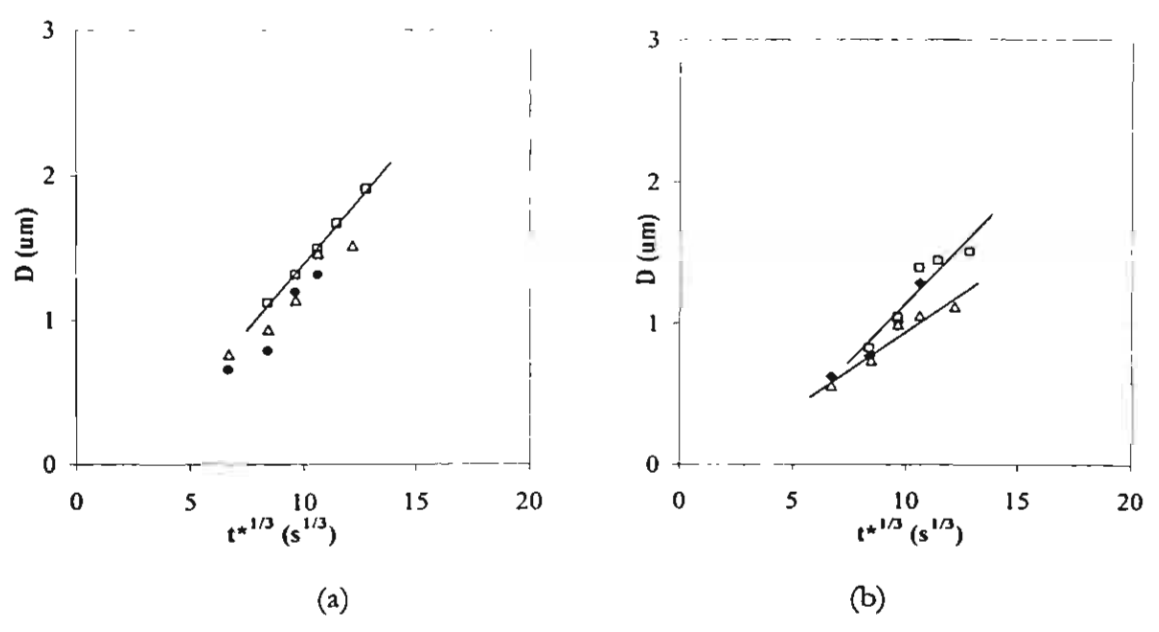


Figure 2.4a Etched domain, D, of morphology of solution blends versus total time in the melt, t\*. Samples annealed at (a) 170°C and (b) 200°C

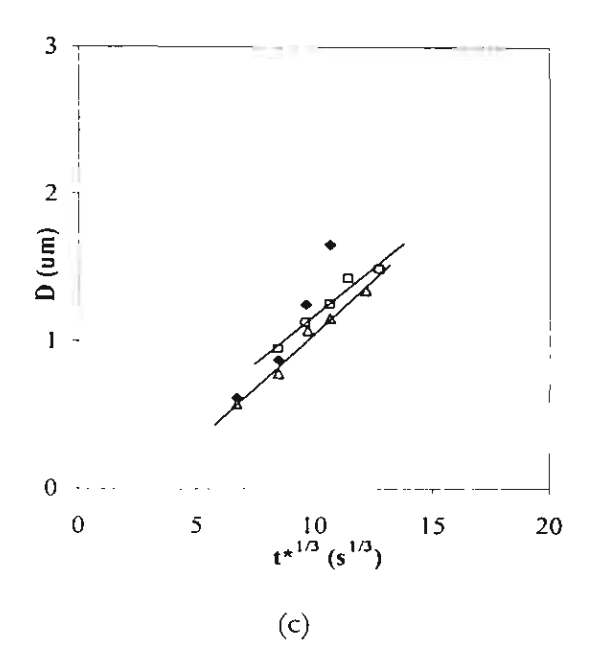


Figure 2.4b Etched domain, D, of morphology of solution blends versus total time in the melt, t\*. Samples annealed at (a) 170°C, (b) 200°C, and (c) 230°C: (◆) un-sheared and sheared at (□) 1 s<sup>-1</sup> and (Δ) 50 s<sup>-1</sup>.

After the annealing times have been corrected, the samples sheared at 1 s<sup>-1</sup> still show coarser morphologies than the unsheared melts and those sheared at 50 s<sup>-1</sup>. Since all samples started with the same, original state the result shows that the coarsening rate is accelerated during shearing at 1 s<sup>-1</sup>, independent of the time spent at this condition. Moreover, the slope of the annealing plots in figure 2.4 are not greatly influenced by shear history indicating that the prior shearing condition did not have a subsequent effect upon the coarsening rate upon cessation of shearing. It may be speculated that at the lower shear rate the stress of dispersion is relatively low and the agitation of the melt increases the probability of domain contact and coalescence.

#### Effect of temperature

Samples were prepared with a shear history comprising a strain of 300 at shear rates of 1 and 50 s<sup>-1</sup>, in addition to unsheared samples, at 170, 200, and 230°C. The domain sizes of these samples during subsequent annealing are plotted as functions of the corrected annealing time, t\*, in figure 2.5. For the unsheared samples there is an equivalence of the effect of annealing time and temperature, since all data fall largely upon a single curve. For the sheared samples, data are separated around curves according to the shearing temperature, that is, there is no equivalence of temperature and time. Apparently, there is an interaction between the effect of shearing and temperature: shearing has a greater effect upon the subsequent coarsening during annealing when shearing is carried out at higher temperatures. This may be a consequence of the partial miscibility of this blend system in which enhanced compatibility is observed at elevated

temperature. Shearing may lead to greater homogenisation of the system resulting in reduced coarsening rates.

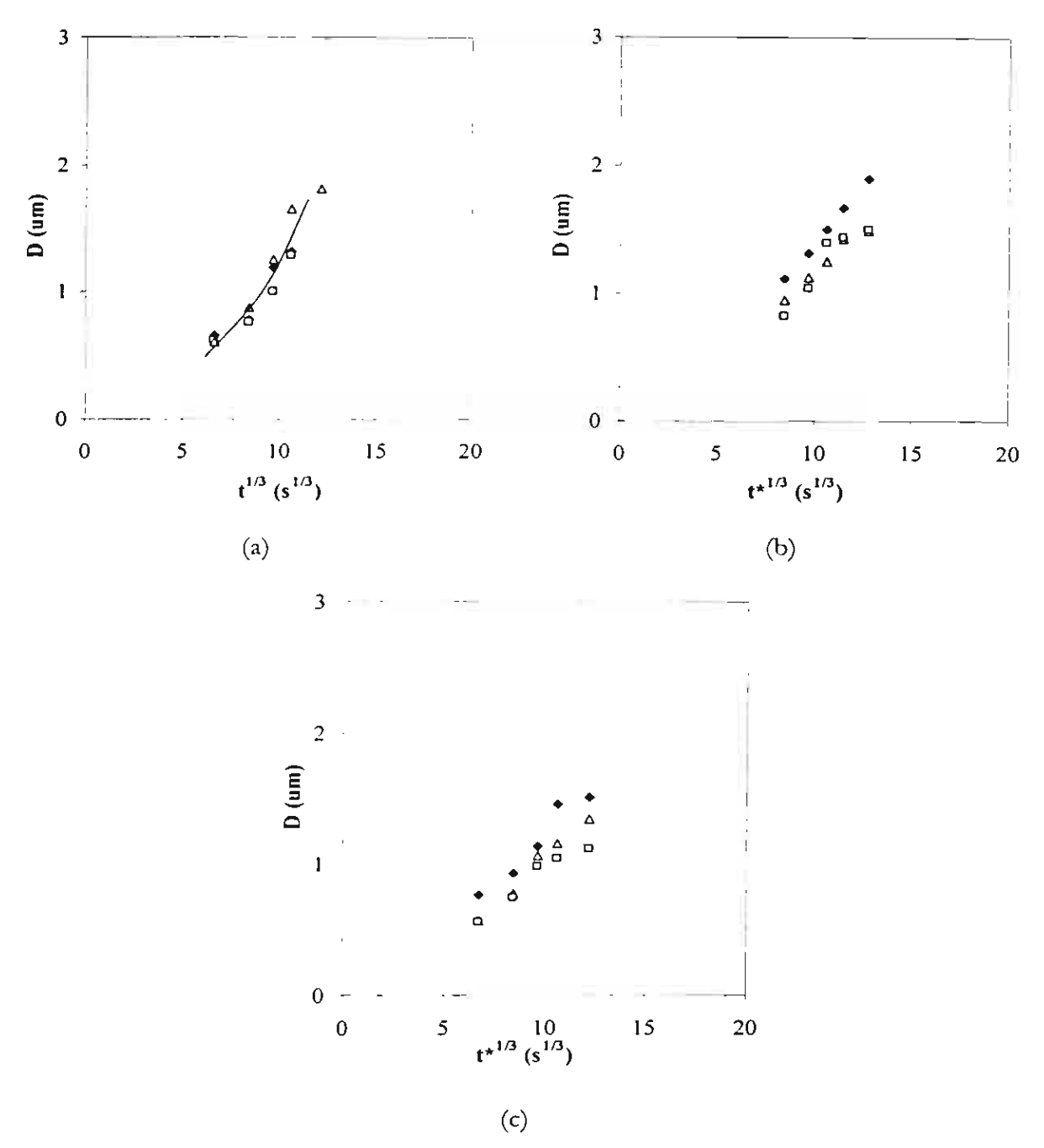


Figure 2.5 Etched domain diameter, D, versus annealing time, t\*, of solution blends (a) no shearing; (b) sheared at 1 s<sup>-1</sup>, and (c) sheared at 50 s<sup>-1</sup> at ( $\spadesuit$ ) 170, ( $\square$ ) 200, and ( $\Delta$ ) 230°C

## Melt extrusion and injection moulded compounds

To investigate the effects of melt temperature and flow history upon the subsequent evolution of morphology in melt processed samples, a series of blends were prepared through

twin-screw extrusion followed by injection moulding. The annealing curves for samples prepared through twin-screw compounding and injection moulding are displayed in figure 2.6 for processing temperatures in the range 150 to 230°C; all samples were annealed at 170°C.

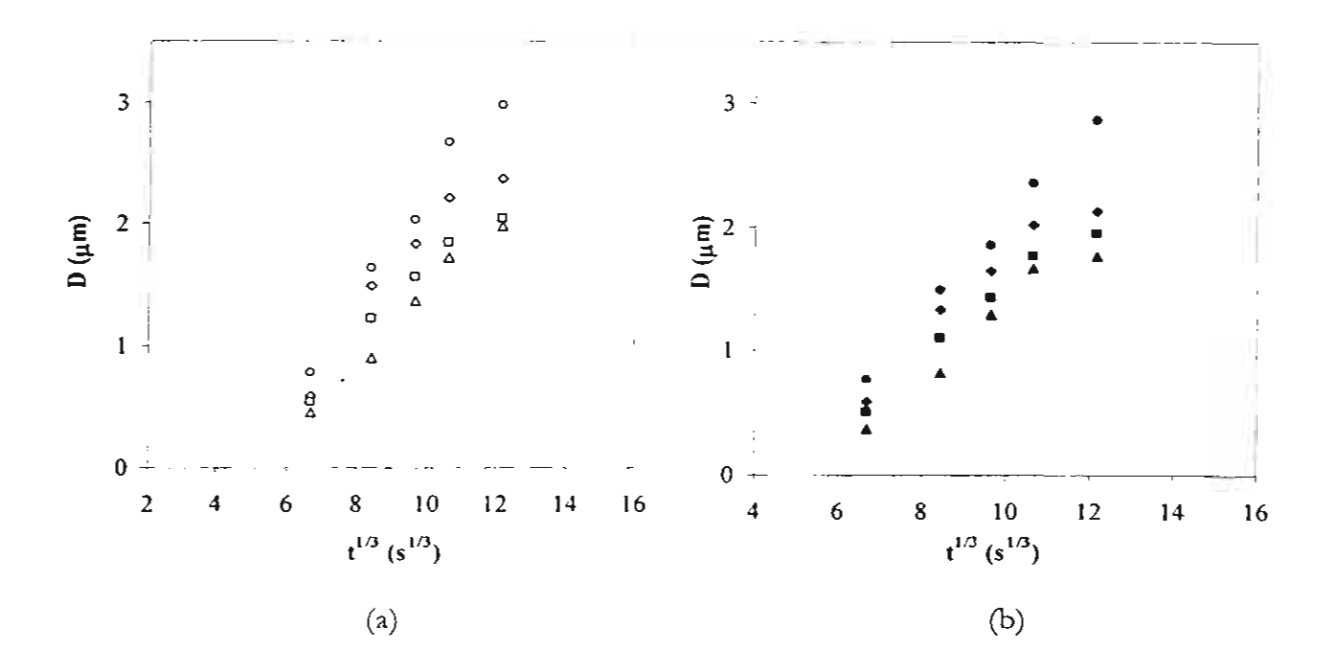


Figure 2.6 Etched domain diameter versus annealing time, t, of melt processed blends: (a) twin screw compound [open symbols] and (b) injection moulded compounds [filled symbols] at  $(0, \bullet)$  150,  $(\lozenge, \spadesuit)$  170,  $(\square, \blacksquare)$  200, and  $(\Delta, \blacktriangle)$  230°C

In this case, elevated processing temperature resulted in reduced coarsening in inverse proportion to the processing temperature. Moreover, this influence of the processing history persisted throughout the subsequent annealing in the quiescent melt-state. The coarsening curves for each temperature are presented in figure 2.7 where the domain sizes are plotted in pairs at different temperatures comparing the coarsening process of the compounds from the twin-screw extruder and the same compound after injection moulding. For comparison, the samples from the twin-screw compounder were heated at the same temperature used to produce the equivalent injection moulding for a time equal to the time spent in the melt during injection moulding. Thus, differences between these curves are caused by the influence of melt flow during moulding, independent of the effects of temperature. Evidently, the action of shearing in the injection-moulding step reduces the coarsening of the compound in subsequent processing.

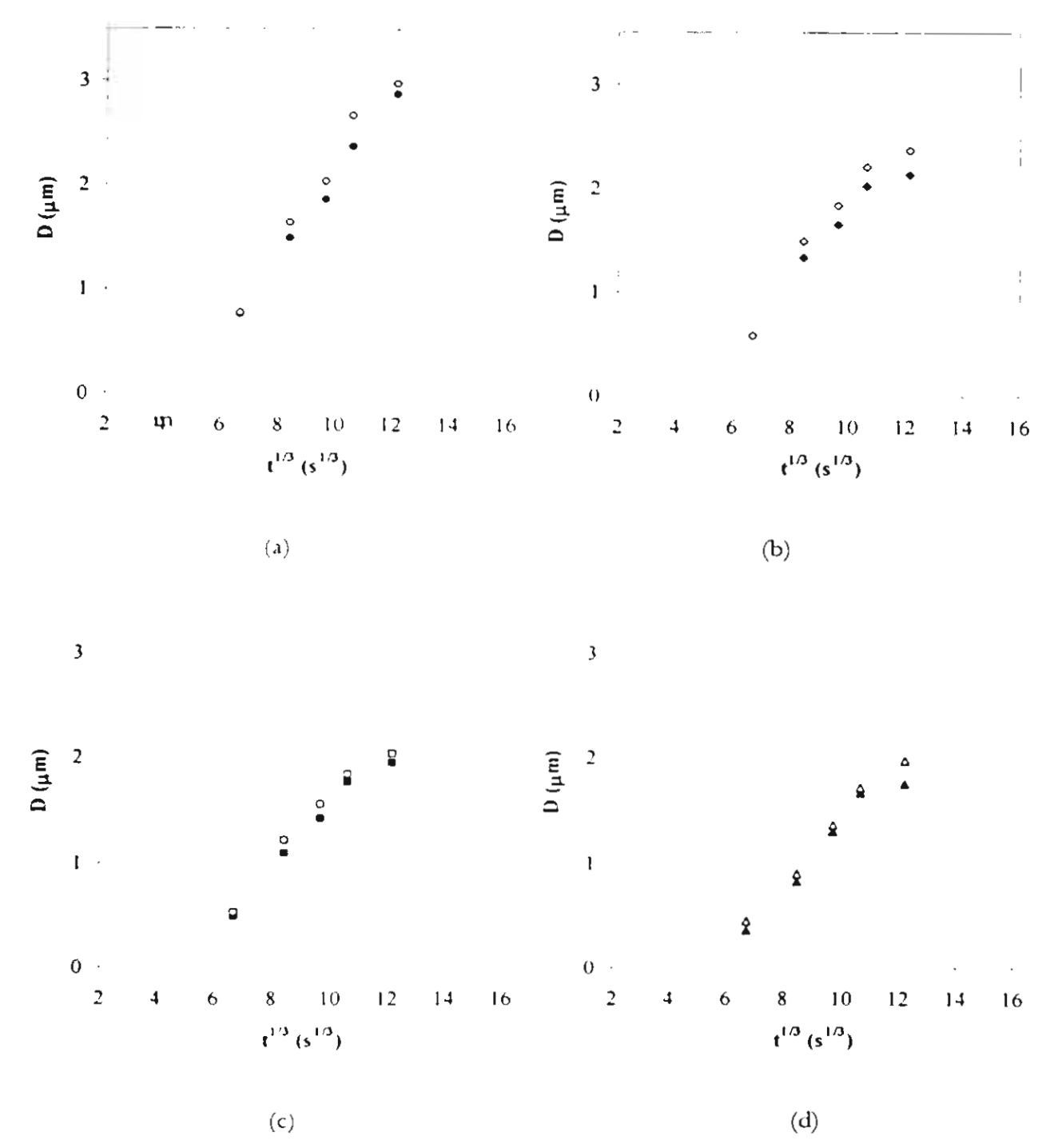


Figure 2.7 Etched domain diameter versus annealing time, t, of melt processed blends: (a) 150, (b) 170, (c) 200, and (d) 230°C. Filled symbols denote injection-moulded compounds whilst the open symbols are for the annealed compounds.

The influence of prior processing temperature may be further considered by scaling the results data assuming equivalence of time and temperature that was found true of the unprocessed solution blends. To this end, the annealing data for the extrusion compounds were scaled in the time component such that the fitted trend lines superimposed at the early stages of coarsening. To accomplish this the annealing times were divided by shift factors of 1, 1.15, 1.35, and 1.8 for

the samples heated at 150, 170, 200, and 230°C, respectively. The shifted data curves are displayed in figure 2.8.

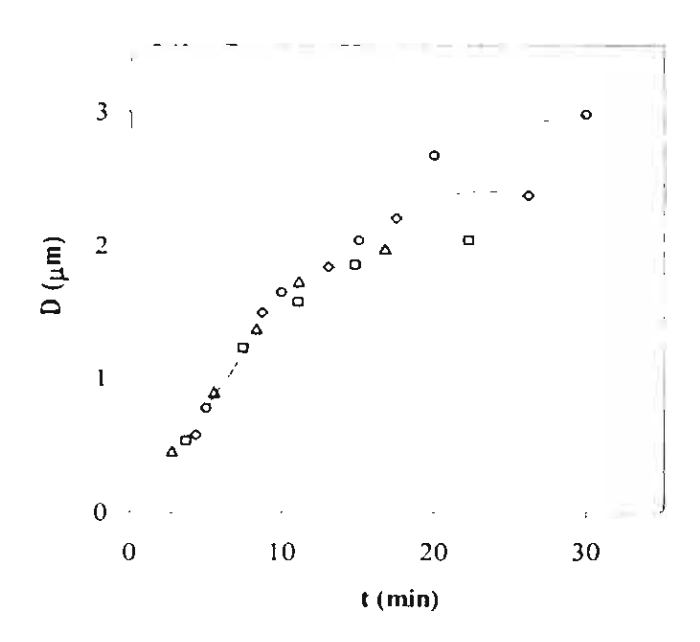


Figure 2.8 Etched domain diameter, D, versus annealing time, t, of twin-screw compounds: (0) 150, (◊) 170, (□) 200, and (Δ) 230°C

Figure 2.8 reveals that when the data superimpose at short annealing times, the curves diverge at longer times. There is not an equivalence of time and temperature in this case. The effect of heating at different temperatures is to change the process of coarsening and is not simply due to differences in melt viscosity.

#### CONCLUSIONS

For the unsheared samples, there was an equivalence of time and temperature upon the coarsening process; that is, higher temperatures and longer annealing time led quantitatively to coarser morphologies. Shearing two-phase melts at 1 s<sup>-1</sup> led to coarsening of the domain morphology at an accelerated rate in comparison with unsheared samples and those sheared at 50 s<sup>-1</sup>. In all cases, conditioning of samples at elevated temperature resulted in reduced coarsening during subsequent annealing. Moreover, the influence of elevated temperature was enhanced through intensive shearing during injection moulding. The short time spent at the elevated temperature has a critical effect upon the morphology that forms in subsequent operations. This effect was not a consequence of changes in melt viscosity, as evidenced by the non-superimposition of the results data when the superposition of time and temperature was assumed.

#### REFERENCES

- 1. A. Tabtiang, B. Parchana, R. A. Venables, and T. Inoue, J. Polym. Sci.: Part B: Polym. Phys., 39(3), (2001)
- 2. J. Wu and Y. W. Mai, Polym. Eng. Sci., 36, 2275 (1996)
- 3. Bates, F. S.; Schulz, M. F.; Rosedale, J. H. Macromolecules 1992, 25, 5547-5550.
- 4. Rhee, J.; Crist B. Macromolecules 1991, 24, 5663-5669.
- 5. Choi, P. Polymer 2000, 41, 8741-8747.
- 6. Krishnamoorti R.; Graessley, W. W.; Balsara N. P.; Lohse, D. J. Macromolecules 1994, 27, 3073-3081.
- 7. Fredrickson, G. H.; Liu, A. J. J Polym Sci Part B: Polym Phys 1995, 33, 1203-1212.
- 8. Yamaguchi, M.; Miyata, H.; Nitta, K. J Appl Polym Sci 1996, 62, 87.
- 9. Thomann, Y.; Suhm, J.; Thomann, R.; Bar, G.; Maier, R. D.; Mulhaupt, R. Macromolecules 1998, 31, 5441.
- 10. Carriere, C. J.; Silvis, H. C. J Appl Polym Sci 1997, 66, 1175.
- 11. Morgan, R. L.; Hill, M.J.; Barham, P. J.; Frye, C. J. Polymer 1997, 38, 1903.
- 12. Hill, M. J.; Barham, P. J. Polymer 1995, 36, 3369.
- 13. Rhee. J.; Crist, B. J Polym Sci Part B: Polym Phys 1994, 32, 159-169.
- 14. Saunders, K. J. Organic chemistry of polymers 2<sup>nd</sup> edition; Chapman and Hall: London, 1988, pp 46-75.
- 15. Chien, J. C. W.; He, D. J Polym Sci Part A: Polym Chem 1991, 29, 1585-1593.

- 16. Halasa, A. F.; Massie, J. M.; Ceresa, R. J. In Science and technology of rubber 2<sup>nd</sup> edition; Mark, J. E.; Erman, B.; Eirich, F. R. editors; Academic Press, San Diego, 1994, p 518.
- 17. De Pooter, M.; Smith, P. B.; Dohrer, K. K.; Bennett, K. F.; Meadows, M. D.; Smith, C. G.; Schouwenaars, H. P.; Geerards, R. A. J Appl Polym Sci 1991, 42, 399-408.
- 18. Carreau, P. J., Rheological equations from Molecular Network Theories, Ph.D. Thesis, University of Wisconsin, 1968.
- 19. Harris, D. C. J Chem Ed 1998, 75, 119.
- 20. Dumoulin, M. M.; Utracki, L. A.; Carreau, P. J. In Two-phase polymer systems; Hanser: Munich, 1991, p 201.
- 21. Crist, B.; Hill, M. J. J Polym Sci Part B: Polym Phys 1997, 35, 2329-2353.
- 22. Cowie, J. M. G. Polymers: Chemistry and physics of modern materials 2<sup>nd</sup> Edition; Blackie Academic and Professional: London, 1991, p 265.
- 23. Bicerano, J. Prediction of polymer properties; Marcel Dekker: New York, 1993, pp 66-70.
- 24. Dehoff, R. T. Quantitative microscopy; McGraw-Hill: New York, 1968, p 131.
- 25. Lee, J. K.; Han, C. D. Polymer 1999, 40, 2521-2536.
- 26. Cahn, J. W. J Chem Phys 1965, 42, 93.
- 27. Inaba, N.; Yamada, T.; Suzuki, S.; Hashimoto, T. Macromolecules 1988, 21, 407-414.
- 28. Bartels, C. R.; Crist, B.; Graessley, M. W. Macromolecules 1984, 17, 2702.
- 29. Cowie, J. M. G. Polymers: Chemistry and physics of modern materials 2<sup>nd</sup> Edition; Blackie Academic and Professional: London, 1991, pp 178-179.
- 30. Bicerano, J. Prediction of polymer properties; Marcel Dekker: New York, 1993, p 286.

### Results Part 3

# The relationship between processing history and the morphology of injection moulded toughened polyolefins

#### From the paper:

Tabtiang T, Parchana B, Venables RA, 'The relationship between processing history and the morphology of injection moulded toughened polyolefins'. Polym.-Plast. Technol. Eng., 40(4), pp.423-436 (2001)

#### Abstract

The solid-state morphologies of three polyolefins, namely isotactic polypropylene (iPP), isotactic poly(propylene-co-ethylene) (iPcE), and high-density polyethylene (PE), toughened with an elastomeric poly(ethylene-co-1-octene) (EOC) have been investigated. Morphologies ranged from dispersed droplets with mean diameters in the range 0.2 to 0.6 µm, for iPP, to a fine interpenetrating morphology comprising 17 nm thick lamella crystals and elastomer-rich regions of length-scale 170 nm when the major component was linear PE. In the iPcE formulations, 10 nm thick lamellar crystals of the matrix polymer were observed in the elastomer domains. Dynamic mechanical analysis and microscopy of quenched and annealed samples showed that each system was phase separated in the solid state and in the melt under quiescent conditions, respectively. The differing solid state morphologies were inferred to result from the mixing under melt flow of the partially miscible polymers during processing and by the subsequent liquid-liquid and solid-liquid phase separation upon cooling.

#### INTRODUCTION

The toughness of plastics modified with a minority elastomer component is critically dependent upon the domain size and morphology of the dispersed phase (1). These factors are influenced by the extent of miscibility of the constituent polymers and the melt processing conditions. Melt stresses and processing time affect the dispersion and coalescence processes; moreover, when the blend components approach the limits of miscibility, the extent of mixing at the molecular level may be affected. The work of Madbouly et al. (3) has shown that flow affects the thermodynamics of miscibility: it was determined that melt flow effected a shift in the glass transition temperatures of polystyrene / poly(vinyl methyl ether) blends in comparison with the same materials that were biphasic at the equal temperature under quiescent conditions. The results were interpreted as an upward shift of the lower critical solution temperature. In the case of polyolefin blends, the heat of mixing is small, and hence the entropy of mixing is relatively

important, in comparison with blends that have enhanced miscibility due to specific interactions. Melt flow may be expected to alter the entropy of the system thereby affecting the mixing (3,4).

In this work, the influence of processing history upon the solid-state morphologies of several injection molded polyolefins containing poly(ethylene-co-1-octene) as the minority elastomer phase has been investigated. Evidence for mixing at the molecular level under melt flow is presented.

#### **EXPERIMENTAL**

Details of the polymer resins used in this work are shown in table 1; MFI is melt flow index, and M<sub>w</sub>, M<sub>n</sub>, and M<sub>z</sub> are the weight, number, and z-average molecular weights, respectively, determined using a Waters gel permeation chromatograph employing polystyrene standards in trichlorobenzene solution at 145°C. N<sub>w</sub> = M<sub>w</sub> / M<sub>n</sub>; i.e., the weight average degree of polymerization and M<sub>n</sub> is the relative molecular mass of the polymer repeat unit. The EOC was compounded with each of the iPP, iPcE, or PE resins, in various weight ratios, using a Prism 16 mm twin screw extruder at a barrel temperature of 180°C and screw speed of 175 rpm. Injection moldings were prepared using a Dr Boy 22S machine, employing barrel temperatures between 170 and 230°C; the mould temperature was 30°C. Plasticization energy, that is the mechanical work applied through the screw was adjusted through control of the back-pressure, in the range 0 to 1.7 MPa, and screw speed, in the range 50 to 150 rpm. Small batches (60 g) were prepared using a Haake Rheocord 90-torque rheometer at 170°C and 50 rpm for 5 min. These samples were used for shearing using a custom-built parallel plate apparatus where the plates could be rapidly demounted such that quenching of the sample in cold water could be carried out.

Shear flow data were generated using a Rosand capillary rheometer and a Haake RT20 parallel-plate rheometer. Charpy impact data were collected using a Zwick pendulum impact tester; specimens were chilled to -10°C in a water / ethylene glycol solution that was cooled using a Neslab RTE111 liquid recirculator or to 0°C in an ice / water slush. Blends of varying composition were annealed in an oil bath, after wrapping in aluminum foil, for 6 hrs at temperatures in the range 140 to 270°C. For higher temperatures the specimens were heated in a tube furnace under nitrogen flow. A thermocouple was inserted in the sample to monitor its temperature. Transmission electron micrographs (TEM) were obtained from RuO<sub>4</sub> vapor stained sections. Unstained sections were viewed with a Nikon E400 transmitted light microscope; the fraction of hexagonal crystals in the iPP samples was determined from the area fraction of highly birefringent spherulites viewed through crossed-polarizing filters. Flat surfaces, prepared with a microtome at -100°C, were treated with a permanganic acid reagent (0.7 w/v% solution at 30°C) (5), to selectively etch the amorphous material, or with toluene at 30°C and viewed using a scanning electron microscope (SEM) after coating with metal.

Table 1. Polymer resins

Polymer resin	Code	Comonomer (mol%)	Density (gcm <sup>3</sup> )	Mw (gmol	Ž	M, (gmol	$M_{\rm w}$ / $M_{\rm n}$	MFI (dgmin <sup>-1</sup> )
Poly(propylene-co-ethylene)	iPcE	S	0.900	214,000	2,240	407,000	3.4	123
Poly(ethylene-co-1-octene)-1	EOC1	7	0.868	172,000	3,506	283,000	5.5	5 <sup>b</sup>
Poly(ethylene-co-1-octene)-2	FOC2	7	0.868	261,000	5,320	389,000	5.1	0.5b
Polypropylene	ddt	0	0.905	291,000	3,725	475,000	9.5	Ō
Polyethylene-1	PET	G :	0.962	128,000	4,563	, ,	, (	185
l'olyethylene-2	1952	С	0.962	000,551	5,525	396,000	3.7	÷

JBS 720A Test condition 12;

<sup>11</sup>BS 720A Test condition 4;

Datum from correlation of MFI with resins of known molecular weight.

MFI is melt flow index.

Ma, Mn, and M, are weight, number, and z-average molecular weights, respectively.

N<sub>w</sub> is weight average degree of polymerization.

Prefix P in 1PP and 1PcE denotes isotactic.

Scanned and calibrated micrographs were quantitatively analyzed using ImagePro software to obtain lamella thickness, area fractions, and mean dispersed domain diameters. All microscopy data presented herein refer to the cores of the samples. Differential scanning calorimeter (DSC) data were obtained with a Perkin Elmer DSC7 instrument: specimens (10 mg ± 0.1 mg) were cut from the central core of the moldings and dipped in silicone to ensure rapid heat transfer to the specimens. Fusion endotherms were obtained at a heating rate of 30°C/min, to limit annealing during heating, under a nitrogen atmosphere. Wide angle X-ray diffraction patterns were collected with a JEOL JDX-350 instrument. Dynamic mechanical analyses were carried out using a Polymer Laboratories DMTA mkII instrument in tensile mode at a deformation frequency of 10 Hz and heating rate of 5°C/min.

#### RESULTS AND DISCUSSION

## Isotactic polypropylene homopolymer formulations

The Charpy impact properties, at 0°C, of the PP / EOC2 (70:30 w/w) compounds, injection molded under various conditions are illustrated in figure 3.1a and 3.1b as functions of mean dispersed phase diameter (determined from micrographs of solvent-etched microtomed surfaces), barrel temperature, and specific mechanical energy input, S<sub>c</sub>.

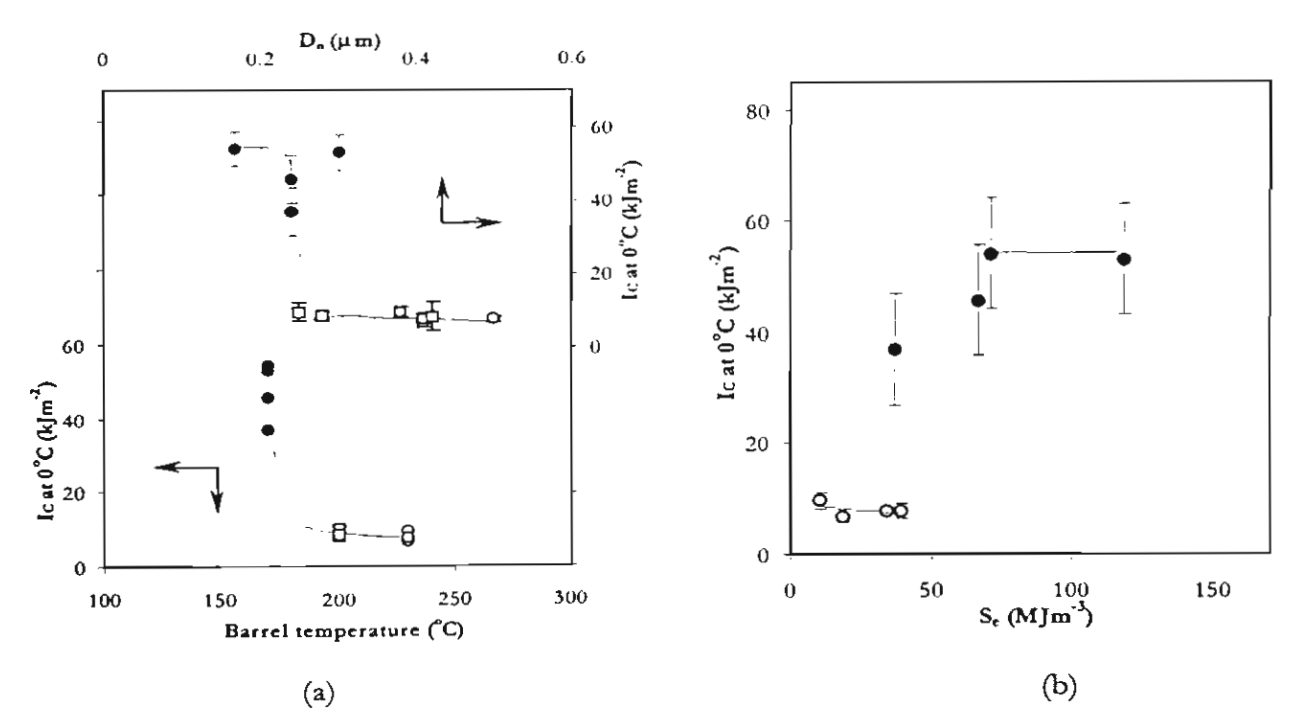


Figure 3.1 Charpy impact energies, I<sub>C</sub>, at 0°C of toughened PP samples containing 30 wt% EOC2. Data are plotted (a) versus mean elastomer domain size and barrel temperature and (b) as a function of plasticization energy, S<sub>e</sub>, during injection molding for samples molded at (●) 170°C, (□) 200°C, and (O) 230°C. Error bars are ± the sample standard deviation.

The power dissipated per unit volume during plasticization, P, was taken as (6):

$$P=\eta(\dot{\gamma})^2,$$

where  $\eta$  is the viscosity at shear rate,  $\dot{\gamma}$ . Shear rate in the channel of screw metering zone was estimated (7)

$$\dot{\gamma} = \frac{\pi DN}{h},$$

where D is the screw diameter, N the screw speed, and h the screw channel depth. Se was calculated

$$S_e = Pt$$

where t is the plasticization time. The impact energies are critically dependent upon the domain size of the elastomer inclusions; a mean domain size of 0.3  $\mu$ m separates low and high toughness groups of samples. This effect in semicrystalline plastics has been explained in terms of a critical inter-particle distance (or ligament length),  $I_d$ , that is a function of the volume fraction of the dispersed domains,  $\phi_d$ , domain size,  $D_n$ , and packing geometry (8):

$$I_d = D_n \left[ \left( \frac{\pi}{6\phi_d} \right)^{\frac{1}{3}} - 1 \right].$$

The model assumes simple cubic packing, and hence the ligament lengths for the molded samples are in the range 35 to 86 nm with a critical value of 61 nm. The mean domain size in the extruded compound, i.e. prior to injection molding, was 0.29 µm. Moldings prepared using the higher barrel temperatures had lower impact toughness, due to the presence of larger elastomer domains, and hence increased ligament lengths. This was presumably due to the enhanced rate of interfacial tension driven droplet coalescence associated with the lower viscosity conditions encountered at high temperature. Plasticization energy had little effect upon the toughness of samples prepared at 230°C, most likely due to the dominance of coalescence at this temperature. Higher plasticization energies, achieved through increasing back pressure and screw speed, when the barrel temperature was 170°C led to enhanced impact toughness. The latter effect may be largely traced to the influence upon domain size with the increased melt stresses counteracting

the coalescence. It was determined through polarized light microscopy that typically the cores of the iPP moldings comprised spherulites of around 10 µm in diameter, 18.0 area% of which were made of the hexagonal and 82.0 area% of monoclinic crystal type. The presence of the hexagonal form was confirmed through X-ray diffractometry; the triclinic form was absent. The average crystallinity, % $\chi$ , through DSC analysis, of all iPP samples prepared was 44.1 wt% from:

$$\%\chi = \Delta H_f \left( \frac{w_{f(\alpha)}}{\Delta H_{(100\alpha)}} + \frac{w_{f(\beta)}}{\Delta H_{(100\beta)}} \right) 100,$$

with a coefficient of variation (CV = standard deviation / mean) of 4.3%;  $w_{f(\alpha)}$  and  $w_{f(\beta)}$  are the fraction of monoclinic and hexagonal spherulites. The heat of fusion for a 100% crystalline iPP in monoclinic form,  $\Delta H_{(100\alpha)}$ , was 207 J/g (9), and the corresponding value for the hexagonal form,  $\Delta H_{(100\alpha)}$ , was 113 J/g (10). CV from replicate samples prepared at 200°C was 2.3%. The average peak melting temperature of all iPP samples, by DSC, was 164°C with a CV of 0.3%; replicate analyses gave a CV for experimental error as 0.2%.

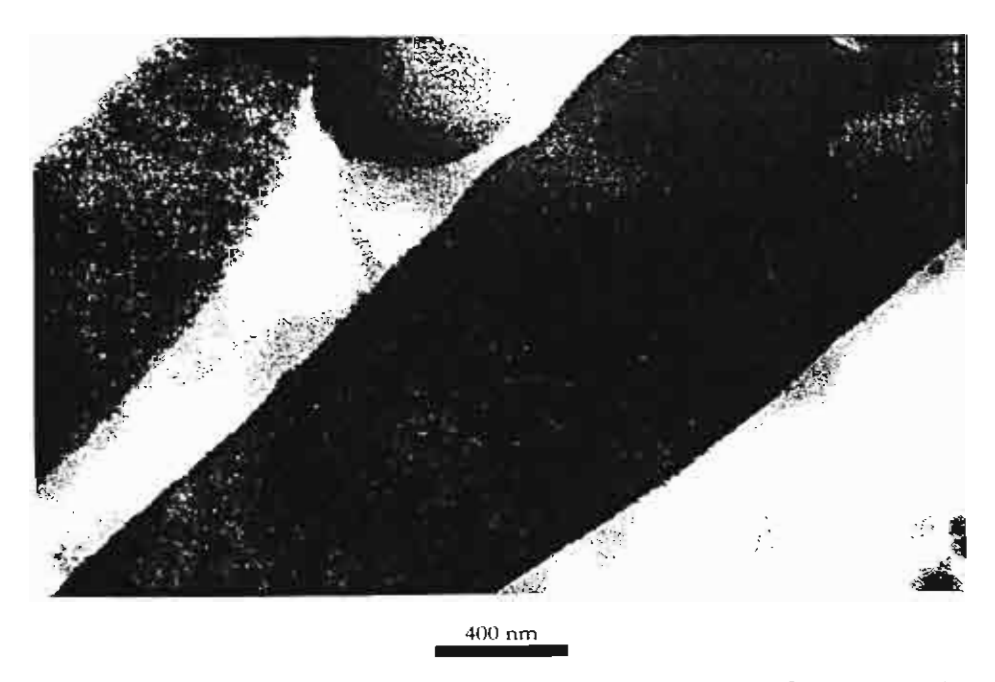


Figure 3.2 TEM micrograph showing the detail of the morphology of a PP sample containing 40 wt% of EOC2. The sample was mixed in an internal mixer, sheared between parallel plates at 230°C, and then quenched. Micrograph shows a section taken at 5 mm from the centre of the sample; at this position, shear rate was 10 s<sup>-1</sup>.

Moreover, Scherrer crystallite size, Ls, calculations from (11)  $L_S = \lambda/(\beta_{hkl}\cos\theta)$  were qualitatively consistent with the melting data; where  $\lambda$  is the wavelength of the x-ray radiation,